Proteolytically cleaved MLL subunits are susceptible to distinct degradation pathways

Akihiko Yokoyama[1,*], Francesca Ficara[2,‡], Mark J. Murphy[2,‡], Christian Meisel[2], Alpana Naresh[2], Issay Kitabayashi[1] and Michael L. Cleary[2,*]

[1]Division of Hematological Malignancy, National Cancer Center Research Institute, Tokyo 104-0045, Japan
[2]Department of Pathology, Stanford University School of Medicine, Stanford, CA 94305, USA
*Authors for correspondence (ayokoyam@ncc.go.jp; mcleary@stanford.edu)
‡These authors contributed equally to this work

Accepted 25 February 2011
Journal of Cell Science 124, 2208-2219

doi:10.1242/jcs.080523

Summary

The mixed lineage leukemia (MLL) proto-oncogenic protein is a histone-lysine *N*-methyltransferase that is produced by proteolytic cleavage and self-association of the respective functionally distinct subunits (MLL^N and MLL^C) to form a holocomplex involved in epigenetic transcriptional regulation. On the basis of studies in *Drosophila* it has been suggested that the separated subunits might also have distinct functions. In this study, we used a genetically engineered mouse line that lacked MLL^C to show that the MLL^N–MLL^C holocomplex is responsible for MLL functions in various developmental processes. The stability of MLL^N is dependent on its intramolecular interaction with MLL^C, which is mediated through the first and fourth plant homeodomain (PHD) fingers (PHD1 and PHD4) and the phenylalanine/tyrosine-rich (FYRN) domain of MLL^N. Free MLL^N is destroyed by a mechanism that targets the FYRN domain, whereas free MLL^C is exported to the cytoplasm and degraded by the proteasome. PHD1 is encoded by an alternatively spliced exon that is occasionally deleted in T-cell leukemia, and its absence produces an MLL mutant protein that is deficient for holocomplex formation. Therefore, this should be a loss-of-function mutant allele, suggesting that the known tumor suppression role of MLL may also apply to the T-cell lineage. Our data demonstrate that the dissociated MLL subunits are subjected to distinct degradation pathways and thus not likely to have separate functions unless the degradation mechanisms are inhibited.

Key words: MLL, Degradation, Proteolysis

Introduction

The mixed lineage leukemia (MLL) protein is an epigenetic transcriptional regulator that is crucial in many developmental and homeostatic processes. It maintains proper Hox gene expression during embryogenesis and hematopoiesis (Jude et al., 2007; McMahon et al., 2007; Yu et al., 1998; Yu et al., 1995) and regulates expression of cyclin-dependent kinase inhibitors (CDKIs) in fibroblasts (Milne et al., 2005). Misregulation of MLL-dependent transcriptional pathways is associated with various pathologies. Gain-of-function mutations of MLL in the hematopoietic lineage result in constitutive expression of Hox genes leading to acute leukemia (Ayton and Cleary, 2001; Hess, 2004; Krivtsov and Armstrong, 2007), whereas loss of the MLL- and MLL2-complexes through mutations of menin, an essential MLL-associated cofactor (Hughes et al., 2004; Yokoyama et al., 2004), leads to decreased expression of CDKIs in the endocrine tissues, hyper proliferation of endocrine cells, and development of multiple endocrine neoplasias (Bertolino et al., 2003; Crabtree et al., 2001; Karnik et al., 2005; Milne et al., 2005). Thus, MLL regulates growth-regulatory transcriptional circuits that are subject to perturbations in various malignancies.

MLL is translated as a large precursor protein that subsequently undergoes proteolytic processing into two fragments (MLL^N and MLL^C) that self-associate through non-covalent interaction to form an intramolecular complex (Hsieh et al., 2003b; Yokoyama et al., 2002). MLL is processed by the Taspase 1 endopeptidase, which specifically cleaves at sites that are evolutionarily conserved with MLL2 and *Drosophila* TRX (Hsieh et al., 2003a; Hsieh et al., 2003b; Yokoyama et al., 2002); however, the biological significance of processing remains unclear. MLL^N appears to comprise a targeting subunit that contains several motifs involved in DNA binding (AT hooks, CXXC domain) (Ayton et al., 2004; Birke et al., 2002; Zeleznik-Le et al., 1994) and chromatin recognition [plant homeodomain (PHD) fingers, bromo domain]. In particular, the third PHD finger (PHD3) was shown to associate with di- or tri-methylated histone H3 lysine 4, which might be regulated by Cyp33 binding (Fair et al., 2001; Chang et al., 2010; Milne et al., 2010; Wang et al., 2010b). PHD3 is not present in the leukemic MLL fusion proteins and diminishes oncogenic ability if artificially included in an MLL fusion protein (Muntean et al., 2008; Chen et al., 2008). MLL^N associates with menin and LEDGF, which are also crucial for linking MLL proteins with target chromatin (Yokoyama and Cleary, 2008). Lastly, binding to MYB and the PAF1 complex is also implicated in the target recognition (Jin et al., 2010; Milne et al., 2010; Muntean et al., 2010). By contrast, MLL^C has features of a transcriptional effecter subunit that possesses a potent transactivation domain (Yokoyama et al., 2002; Zeleznik-Le et al., 1994) and a methyltransferase (SET) domain specific for lysine 4 of histone H3, an epigenetic mark associated with transcriptionally active states (Milne et al., 2002; Nakamura et al., 2002). The SET domain also associates with accessory factors (WDR5, RBBP5 and ASH2L) that promote optimal substrate recognition and enzymatic activity (Dou et al., 2006; Steward et al., 2006; Southall et al., 2009; Yokoyama et al., 2004). Intramolecular interaction is mediated in part by the FYRN (also called ATA1) and FYRC (also called ATA2) domains (Caldas et

al., 1998; Hsieh et al., 2003b; Yokoyama et al., 2002), which directly associate with each other (Garcia-Alai et al., 2010; Hsieh et al., 2003b; Pless et al., 2011). Thus, the MLL complex is thought to consist of an MLL^C effecter subunit tethered to the MLL^N targeting subunit by non-covalent association. This model has prompted the hypothesis that conditional association or disassociation of the MLL^C subunit might serve important roles in MLL-dependent transcriptional regulation. Supporting this hypothesis, a genome-wide association analysis in *Drosophila* showed that TRX^N and TRX^C could differently localize at some loci (Schuettengruber et al., 2009).

In this study, we analyzed in vivo roles of the MLL^N–MLL^C holocomplex (hereafter referred to as MLL holocomplex) by engineering a knock-in mouse line in which the MLL^C effecter subunit cannot be produced. Our results show that the MLL holocomplex is responsible for MLL-dependent transcription in various developmental processes. We found that dissociated MLL subunits are subjected to distinct degradation pathways and therefore are not expected to have functions unless the degradation pathways are inhibited. A genetic lesion associated with human T-cell leukemias disables holocomplex formation and thus is expected to abolish MLL-dependent transcription, raising the possibility of a tumor suppressor role for MLL in the lymphoid lineage.

Results

MLL^C is required for MLL-dependent transcription and the stability of MLL^N during embryogenesis

To investigate the role of the MLL^C subunit in vivo, we generated a knock-in mouse line with a stop codon introduced at the second processing site, thereby exclusively expressing MLL^N (Fig. 1A,B). Diagnostic genomic PCR and sequencing of the PCR product confirmed that recombined embryonic stem (ES) cells harbored the targeted allele (Fig. 1C,D). Western blotting analysis confirmed the lack of MLL^C expression in *dC* homozygous ($Mll^{dC/dC}$; hereafter referred to as *dC/dC*) embryos (Fig. 1E). However, expression of the MLL^N fragment was severely reduced, indicating that MLL^N is unstable without MLL^C, as previously suggested (Hsieh et al., 2003b). *dC/dC* embryos died during gestation at embryonic day

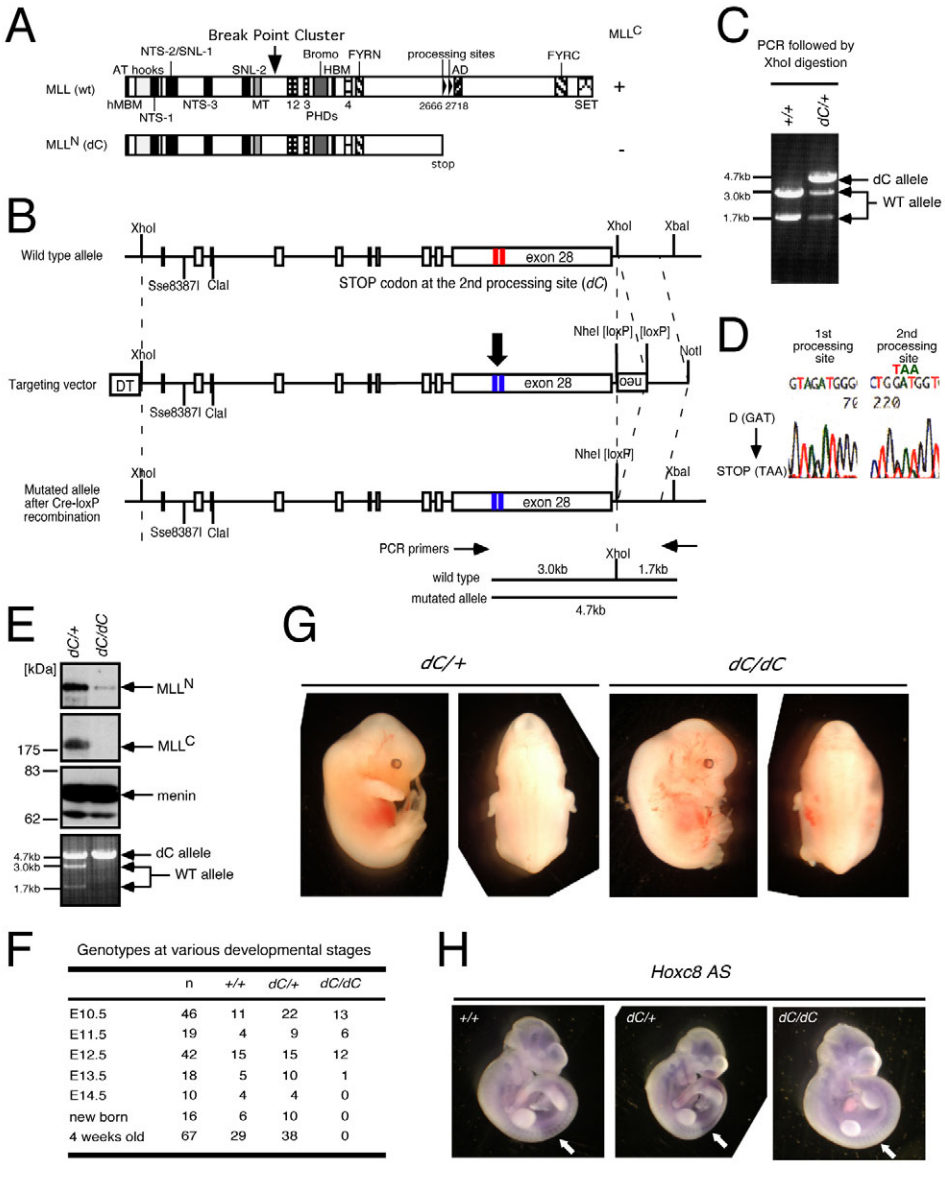

	n	+/+	dC/+	dC/dC
E10.5	46	11	22	13
E11.5	19	4	9	6
E12.5	42	15	15	12
E13.5	18	5	10	1
E14.5	10	4	4	0
new born	16	6	10	0
4 weeks old	67	29	38	0

Fig. 1. MLL^C is required for MLL-dependent transcription during embryogenesis. (**A**) Schematic representations of dC-mutant MLL proteins. (**B**) The structure of the targeting vector. The positions of diagnostic primers are shown at the bottom. (**C**) Successful recombination of positive ES clones was confirmed by PCR followed by digestion with *Xho*I. The *Xho*I site downstream of exon 28 was destroyed in the recombined allele as shown in B. (**D**) Sequences of PCR fragments amplified from genomic DNAs of the recombined ES clones. (**E**) Expression of MLL proteins in embryos at E11.5. Whole-embryo extracts were immunoblotted with anti-MLL^N (mmN4.4), anti-MLL^C (9–12) or anti-menin antibody. The diagnostic PCR data are shown in the bottom panel. (**F**) Genotypes at various developmental stages. The numbers of embryos or mice with the indicated genotypes are shown for each developmental stage. Viability was confirmed by presence of a beating heart. (**G**) Abnormal features of *dC/dC* embryo at E12.5. (**H**) Expression of *Hoxc8* transcripts in E10.5 embryos. Whole-mount in situ hybridization was performed using antisense *Hoxc8* probes (*Hoxc8* AS). Arrows indicate positions of target gene expression.

(E) 13–14 manifesting subcutaneous edema, hemorrhage and hunched posture (Fig. 1F,G), similar to the phenotypes reported in mice with other *Mll*-truncating mutations (Yagi et al., 1998; McMahon et al., 2007) and failed to maintain *Hoxc8* expression at E10.5 (Fig. 1H). Thus, the MLL holocomplex is required for embryogenesis.

Loss of MLL^C causes post-transcriptional degradation of MLL^N and p53-dependent premature senescence in fibroblasts

To further analyze the effects of the loss of MLL^C on MLL-dependent transcription, we established wild type (wt) and *dC/dC* mouse embryonic fibroblast (MEF) cell lines. Despite the comparable *Mll* mRNA levels, MLL^N protein in *dC/dC* MEFs was not detectable, indicating that MLL^N is degraded by a post-transcriptional mechanism (Fig. 2A,B). Expression of MLL target genes including *Hoxc8*, *Hoxc9*, *Cdkn2c* and *Cdkn1b* was severely impaired in *dC/dC* MEFs, whereas *Hoxc4* was unaffected (Fig. 2B). The mRNA sequence downstream of the artificially introduced stop codon was equally abundant as that of the upstream counterpart, and the ratios of the N-terminal and C-terminal portions of the *Mll* mRNA were comparable between *dC/dC* and the wild-type control MEFs (Fig. 2C). *dC/dC* MEFs displayed a premature senescence phenotype both in a proliferation assay and in a 3T3 senescence assay (Fig. 2D,E) consistent with a previous human fibroblast study (Caslini et al., 2009). Moreover, *PAI-1* (*Serpine 1*), a well-known senescense inducer (Kortlever et al., 2006), was expressed at high levels in *dC/dC* MEFs, whereas *Pml*, another senescence inducer, was

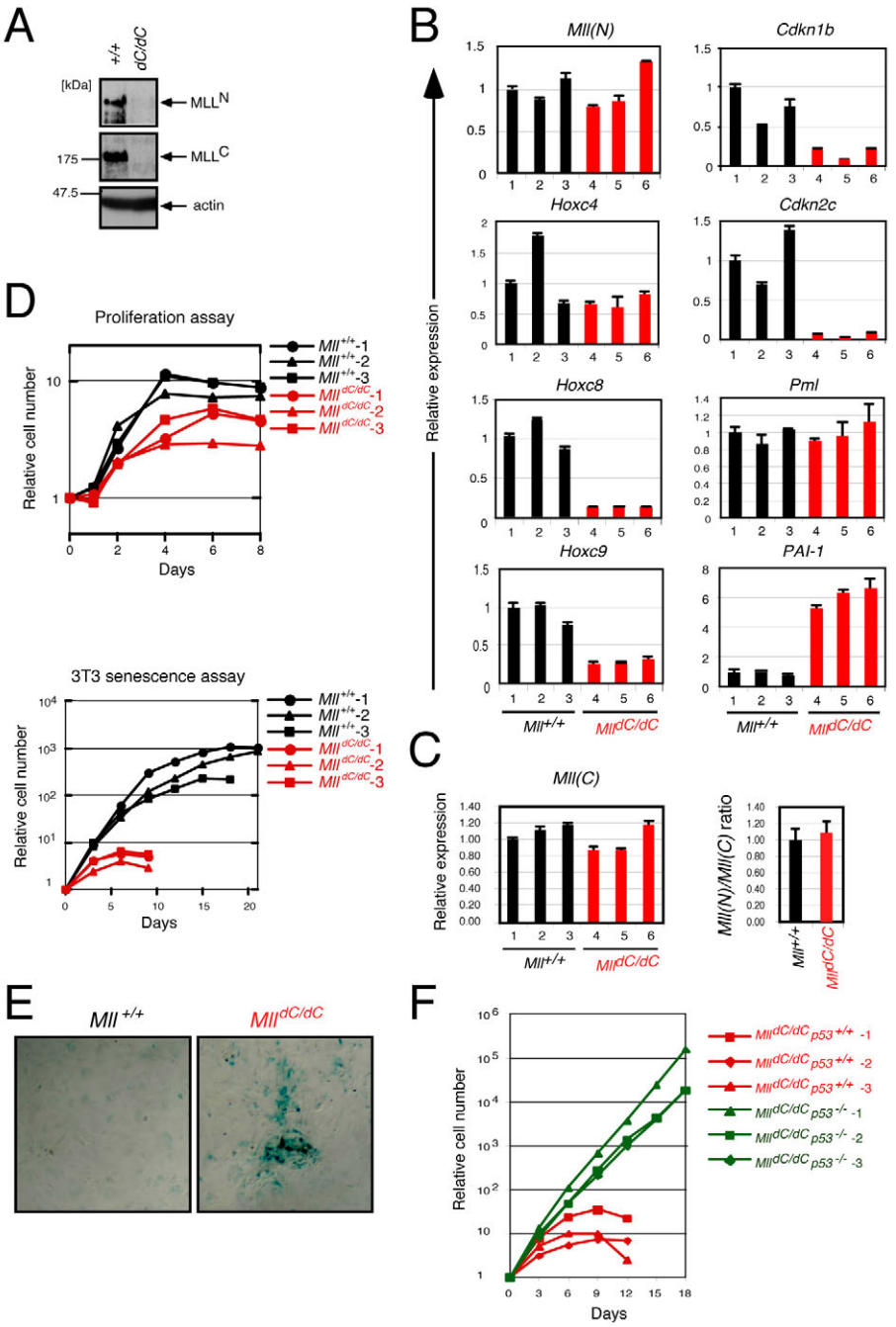

Fig. 2. The MLL holocomplex is required for MLL-dependent transcription in MEFs. (**A**) Protein expression of the MLL subunits in MEFs. Cell lysates prepared from wt or *dC/dC* MEFs were immunoblotted with anti-MLL^N (mmN4.4), anti-MLL^C(9–12) or anti-actin antibody. (**B**) Expression of various genes in *dC/dC* MEFs. Three independently established lines for the indicated genotypes were examined by quantitative RT-PCR for the genes indicated at the top of each panel. RNA was prepared from the third passage MEFs before they went into senescence. Relative expression levels (normalized to *Gapdh*) of various transcripts are depicted relative to those of clone #1, which were arbitrarily set as 1. Error bars represent the standard deviations of triplicate PCRs. (**C**) Expression of *Mll* was analyzed using a qPCR probe for a coding sequence downstream of the processing site as in B. The ratios of the *Mll* mRNA signal detected by the probe upstream of the processing site (N) toward that by the probe downstream of the processing site (C) are shown in the right panel. (**D**) Proliferation and 3T3 senescence assays were performed on wt and *dC/dC* MEFs. MEFs were analyzed after the third passage. A representative result, in which three clones each for the two genotypes were analyzed in a single experiment, is shown. Different clones were also analyzed and reproducibly showed a similar result. (**E**) Senescence-associated β-galactosidase assay of wt or *dC/dC* MEFs. (**F**) Proliferation and 3T3 senescence assays were performed for three lines each of *dC/dC* MEFs with or without homozygous p53 knockout alelles. MEFs were analyzed after the third passage.

unaffected (Fig. 2B). MEFs harboring homozygous *dC* and *p53* null-mutations proliferated without going into senescence (Fig. 2F). Thus, the senescence triggered by loss of MLL^C is p53 dependent. These results demonstrate that loss of MLL^C leads to destruction of MLL^N in vivo and abolishes MLL-dependent transcription to cause p53-dependent premature senescence in MEFs.

MLL^C is required for maintenance of hematopoietic stem cells and progenitors in fetal hematopoiesis

The role of the MLL holocomplex in hematopoietic development was analyzed in E12.5 embryos because previous studies have shown that MLL affects fetal hematopoiesis (Ernst et al., 2004; McMahon et al., 2007; Yagi et al., 1998) (Fig. 3A). The livers of *dC/dC* embryos were hypocellular compared with wt and heterozygous counterparts (Fig. 3B). The relative frequency of LKS (Lin^+, Kit^+, $Sca1^+$) cells, which include hematopoietic stem cells (HSCs) and multipotent progenitors (MPPs), and common myeloid progenitors (CMPs) was severely reduced in *dC/dC* fetal livers but was partially restored at the granulocyte–monocyte progenitor (GMP) or megakaryocyte–erythroid progenitor (MEP) stages (Fig. 3C,D), indicating that MLL is particularly required for the maintenance of HSCs, MPPs and CMPs at E12.5. Interestingly, MPPs ($CD48^+$ LKS), rather than HSCs ($CD48^-$ LKS), were the most affected cells. In particular, the relative frequency of $CD48^+$ $Flk2^+$ LKS cells was severely decreased in *dC/dC* fetal livers compared with control livers (nearly to 1/100 of the control), whereas HSCs were reduced by ~70%. These results suggest that the MLL holocomplex is required for the expansion of not only HSCs but also MPPs.

Despite the severe defects in the early hematopoietic cell compartments, *dC/dC* fetal livers contained highly differentiated hematopoietic cells including Mac-1^{hi} populations (Fig. 3C,D), which express the Mac-1 macrophage marker at high levels, and enucleated red blood cells (Fig. 3E). Moreover, *dC*/*dC* fetal liver cells differentiated into functional macrophages when cultured in the presence of granulocyte-macrophage colony stimulating factor (GM-CSF) in vitro (Fig. 3E), indicating that the potential for hematopoietic differentiation was preserved, which is consistent with previous studies of *Mll*-deficient mice (Yagi et al., 1998). Thus, the MLL holocomplex is not required for myeloid–erythroid differentiation. Nevertheless, transplantation of *dC/dC* fetal liver cells into lethally irradiated recipients failed to reconstitute the hematopoietic system, whereas one-tenth the dose of control fetal liver cells was sufficient to successfully reconstitute the system (Fig. 3F), revealing a profound functional deficiency similar to that observed in *Mll* knockout fetal liver and adult bone marrow (Jude et al., 2007; McMahon et al., 2007). Recipients of *dC/dC* fetal liver cells died 3–4 weeks after transplant, consistent with a defect in early progenitors, besides HSCs. This phenotype could not be rescued by the p53-null mutation, indicating that the hematopoietic defects caused by *Mll* mutations are not caused by p53-dependent senescence of hematopoietic progenitors (Fig. 3G). Taken together these results show that MLL^C is required for the proper expansion of hematopoietic stem cells and/or progenitors but not for differentiation.

MLL^C associates with MLL^N through PHD1, PHD4 and the FYRN domain to protect MLL^N from the FYRN-targeted destruction pathway

Next we investigated the molecular mechanism of MLL holocomplex formation and degradation of MLL^N. Previously, the N-terminal intramolecular interaction domain (NIID) was tentatively located in a large region of MLL^N containing the PHD fingers, bromo domain, HCF binding motif and FYRN domain (Yokoyama et al., 2002). It has been shown that the FYRN domain directly associates with MLL^C in in vitro pull down assays (Hsieh et al., 2003b). To determine the mechanisms of intramolecular interaction, a series of MLL^N deletion and substitution mutants (MLL 1/2254 mutants) was examined for their ability to interact with MLL^C (Fig. 4A; supplementary material Fig. S1). Immunoprecipitation (IP) analysis revealed that PHD1 and PHD4 are required for intramolecular interaction, in addition to the FYRN domain (Fig. 4B; supplementary material Fig. S1). The three mutants deficient for MLL^C binding were capable of binding to HCF-1, arguing against the possibilities of abnormal folding of these mutants (supplementary material Fig. S2A,B). Among the three mutants, the ΔPHD1 and ΔPHD4 mutants were unstable compared with those that associate with MLL^C (Fig. 4A). However, the FYRN deletion mutant was as stable as the wt (MLL 1/2254) despite the inability to associate with MLL^C, suggesting that the FYRN domain mediates not only MLL^C interaction but also degradation of MLL^N. Similar results were obtained using full-length MLL internal deletion and substitution mutants (supplementary material Fig. S3A,B) and serial C-terminal deletion mutants of MLL^N (supplementary material Fig. S3C,D). Furthermore, expression levels of MLL^N and MLL^C within a single cell were analyzed by transiently expressing various MLL mutant proteins tagged with CFP and YFP at the N- and C-termini, respectively (all of the mutants lacked the C-terminal intramolecular interaction domain [CIID: 3607–3742aa] encompassing the FYRC domain, so that the processed fragments should dissociate from each other). Flow cytometry analysis showed that the MLL^N fragment lacking the FYRN deletion was more stable than the ΔPHD1 or ΔPHD4 mutants (Fig. 4C; supplementary material Fig. S1).

To assess the destabilizing potential of the FYRN domain in the context of MLL oncoproteins, an artificial oncogenic protein, MLL–AF9, was engineered to contain the FYRN domain, and tested for its oncogenic and transcriptional activities in a myeloid progenitor transformation assay (Fig. 4D,E; supplementary material Fig. S1). The FYRN domain markedly destabilized MLL–AF9 and MLL5′ (Fig. 4F). Furthermore, MLL–FYRN–AF9 was unable to sustain enhanced serial replating capacity unlike MLL–AF9, or maintain expression of MLL target genes such as *Hoxa9* despite an intact AF9 portion and adequate transcription (Fig. 4E). Thus, the FYRN domain is sufficiently potent to destabilize and inactivate MLL oncoproteins. These results indicate that there is an intrinsic FYRN-targeted destruction pathway that destabilizes proteins with an exposed FYRN domain. Hence, intramolecular interaction of MLL^N and MLL^C is necessary not only for their holocomplex formation but also for the protection of MLL^N from its specific destruction mechanism, by masking the FYRN domain.

Deletion of PHD1 sequences encoded by exon 11 of *MLL* abolishes MLL holocomplex formation and leads to destabilization of MLL^N

Deletion of exon 11 of *MLL* [NM_005933 region 4242–4355; formerly described as ‘exon 8’ by Lockner et al. (Lockner et al., 1996)] causes in-frame fusion to produce a variant protein lacking 38 amino acids (Fig. 5A). Alternative splicing that deletes exon 11 occurs at low levels in normal cells and is aberrantly increased in some cases of acute lymphoblastic leukemia (Löchner et al., 1996; Nam et al., 1996). Because exon 11 spans part of PHD1, we tested,

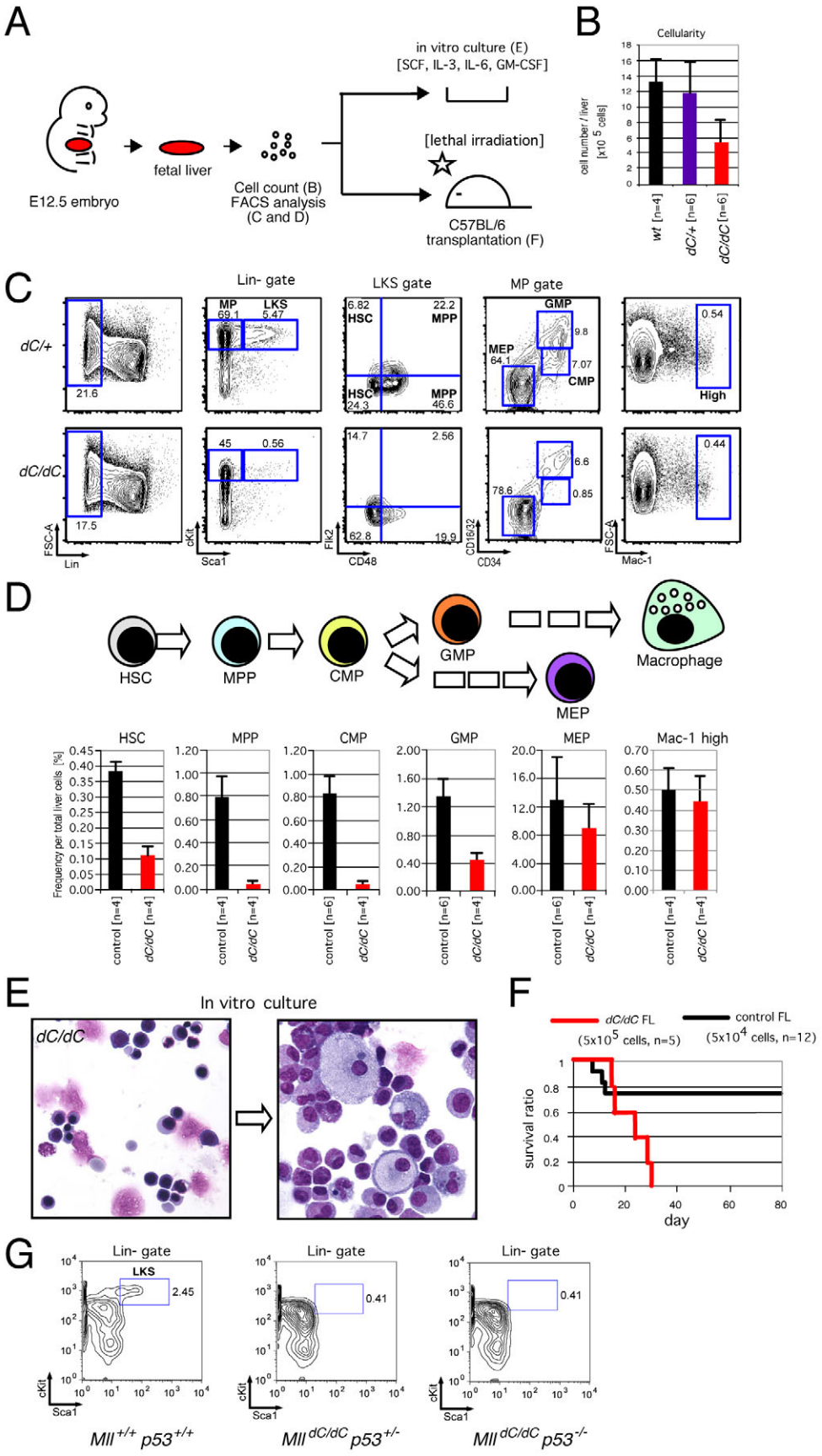

Fig. 3. The MLL holocomplex is required for HSC maintenance and expansion of hematopoietic progenitors, but not for differentiation. (**A**) The experimental scheme of B–F. (**B**) Cellularities of dC mutant fetal livers. Error bars represent the standard deviation of cell numbers of 4 or 6 livers. (**C**) Representative FACS profiles of E12.5 fetal liver cells. Lineage cocktail (anti-CD3, -CD4, -CD8, -B220, -TER119 and -Gr-1) was used to define lineage negative fractions. A marked decrease in the LKS and multipotent progenitor populations was observed in *dC/dC* livers. HSCs are defined as $CD48^{-}$ within the LKS gate where MPPs are defined as $CD48^{+}$ in this study (Christensen and Weissman, 2001; Kim et al., 2006). It should, however, be noted that an alternative model has also been proposed (Mansson et al., 2007). (**D**) Average frequencies of various hematopoietic cell sub-populations per total liver cells. Controls include wt and *dC/+*. The number of embryos analyzed is indicated below. (**E**) The morphology of *dC/dC* fetal liver cells. Enucleated red blood cells were present in *dC/dC* fetal livers. Functional macrophages with engulfed materials emerged after 1 week in culture in methylcellulose medium containing GM-CSF, SCF, IL-3 and IL-6. (**F**) The ability of dC mutant fetal liver cells to reconstitute the hematopoietic system. Fetal liver cells (5×10^5) from *dC/dC* embryos (n=5) or control embryos (5×10^4; n=12) were injected into lethally irradiated recipients. The survival ratio during the monitoring period (80 days) is shown. (**G**) Hematopoietic defects of dC mutants are not caused by p53-dependent senescence. FACS plots of the fetal liver cells, with the various genotypes indicated below, are shown using the lineage cocktail, cKit and Sca1 antibodies.

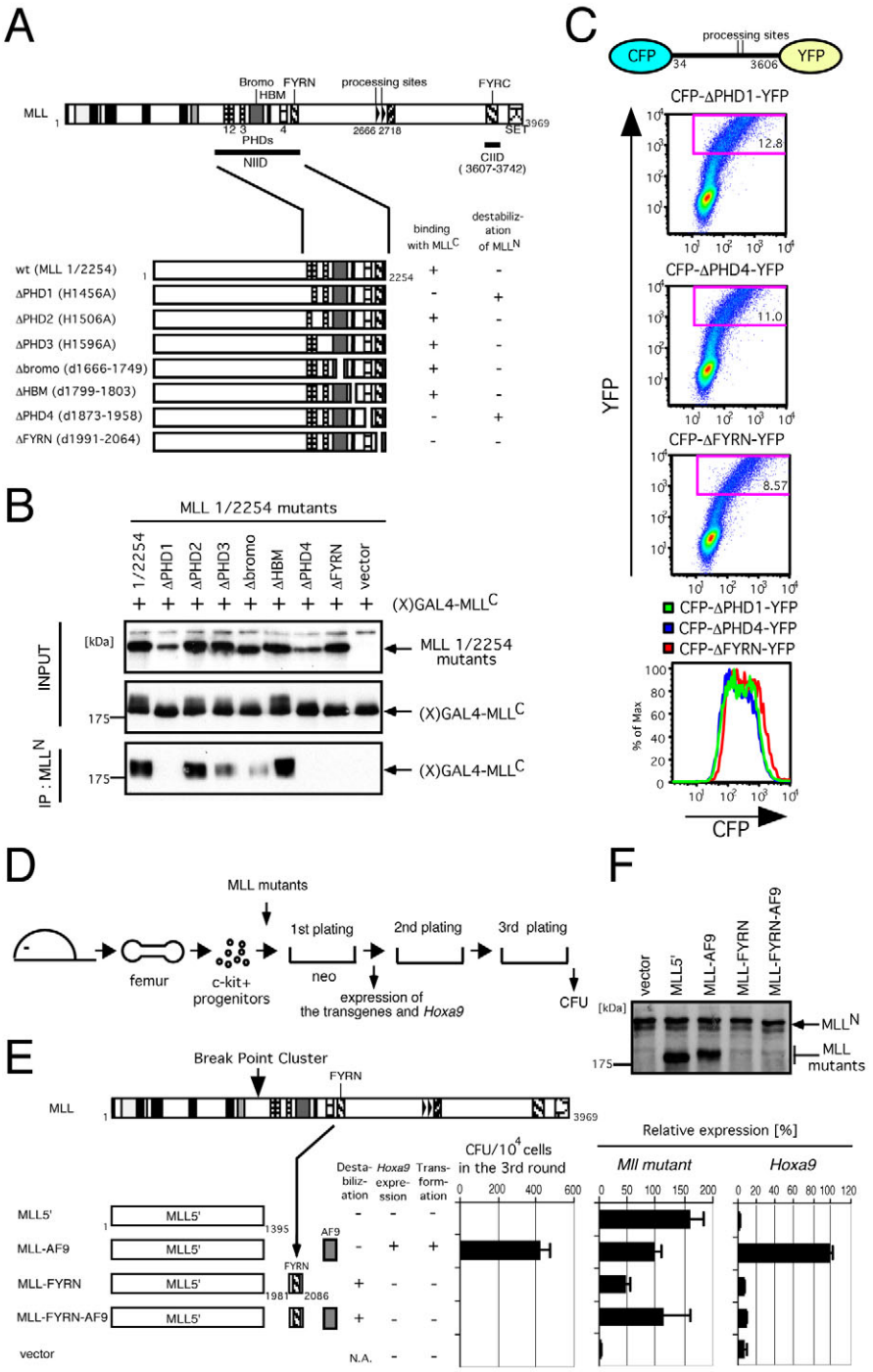

Fig. 4. PHD1 and PHD4 are required for intramolecular interaction in addition to FYRN, which also serves as a destabilization signal. (**A**) Schematic presentation of the various MLL 1/2254 substitution and deletion mutants analyzed. The binding property with MLL^C and susceptibility to destabilization are shown on the right. (**B**) Immunoprecipitation (IP) and western blotting analysis was performed for various MLL 1/2254 mutants that express residues 1–2254 with the indicated substitution and deletion mutations. MLL 1/2254 mutants were coexpressed with Xpress-tagged GAL4-MLL^C [(X)GAL4-MLL^C] in 293T cells. The cell extracts were subjected to IP with anti-MLL^N (mmN4.4) antibody followed by immunoblotting. The precipitates and input samples indicated on the left were immunoblotted with anti-MLL^N (mmN4.4; top panel) and/or anti-Xpress (middle and bottom panels) antibodies. (**C**) Various CFP–MLL 34/3606–YFP mutants were transiently expressed in 293T cells and analyzed by flow cytometry. A population that highly expressed YFP was gated and shown in overlay histograms for its CFP expression level. (**D**) The experimental scheme for the myeloid progenitor transformation assay. Expression of *Hoxa9* was analyzed at the end of the first round of plating. Colony forming units (CFUs) were measured at the end of the third round plating. (**E**) Schematic representation of the MLL–AF9 mutants with or without an FYRN domain. The destabilization property, *Hoxa9* expression, and transformation ability are summarized. CFUs per 10^4 cells at the third round are shown, with error bars representing the standard deviations from three independent analyses. Relative expression levels (normalized to the β-actin gene) of *Mll* mutant and *Hoxa9* transcripts in the first round colonies are depicted relative to MLL–AF9-transduced cells arbitrarily set as 100 (%). Quantitative PCR was performed with specific primers and probes for human *MLL* (which detects various *MLL* mutants but not endogenous mouse *Mll*) or mouse *Hoxa9* and standardized to the β-actin gene. (**F**) Protein expression of various FYRN mutants. MLL–AF9 mutants fused with or without an FYRN domain were expressed in plat-E cells and immunoblotted with anti-MLL^N antibody (mmN4.4).

using IP analysis, whether an exon 11 deletion mutant of MLL (designated Δexon11) forms an MLL^N–MLL^C holocomplex. Exon 11 deletion completely abolished MLL^N–MLL^C intramolecular interaction both when two fragments were separately expressed (Fig. 5B; supplementary material Fig. S1) and in the full-length context (Fig. 5C; supplementary material Fig. S1). Furthermore, the Δexon11 mutant was unstable compared with the FYRN deletion mutant (Fig. 5B–D; supplementary material Fig. S1), analogous to the ΔPHD1 and ΔPHD4 mutants (Fig. 4C). Thus, the *MLL* exon 11 deletion mutation associated with leukemia disrupts intramolecular interaction and thereby destabilizes MLL^N.

Free MLL^C is exported to the cytosol and degraded by the proteasome

Next, we investigated the biological properties of the MLL Δexon11 mutant and its processed fragments. Following proteolytic processing, MLL^N and MLL^C normally colocalize in the nucleus as components of the MLL holocomplex (Fig. 6A; supplementary material Fig. S1). However, exogenously expressed MLL^C localized exclusively in the cytosol, whereas exogenous MLL^N resided predominantly in the nucleus (Fig. 6A). Covalent fusion of MLL with the GAL4 DNA binding domain, which contains potent nuclear localization signals (Silver et al., 1984), only partially

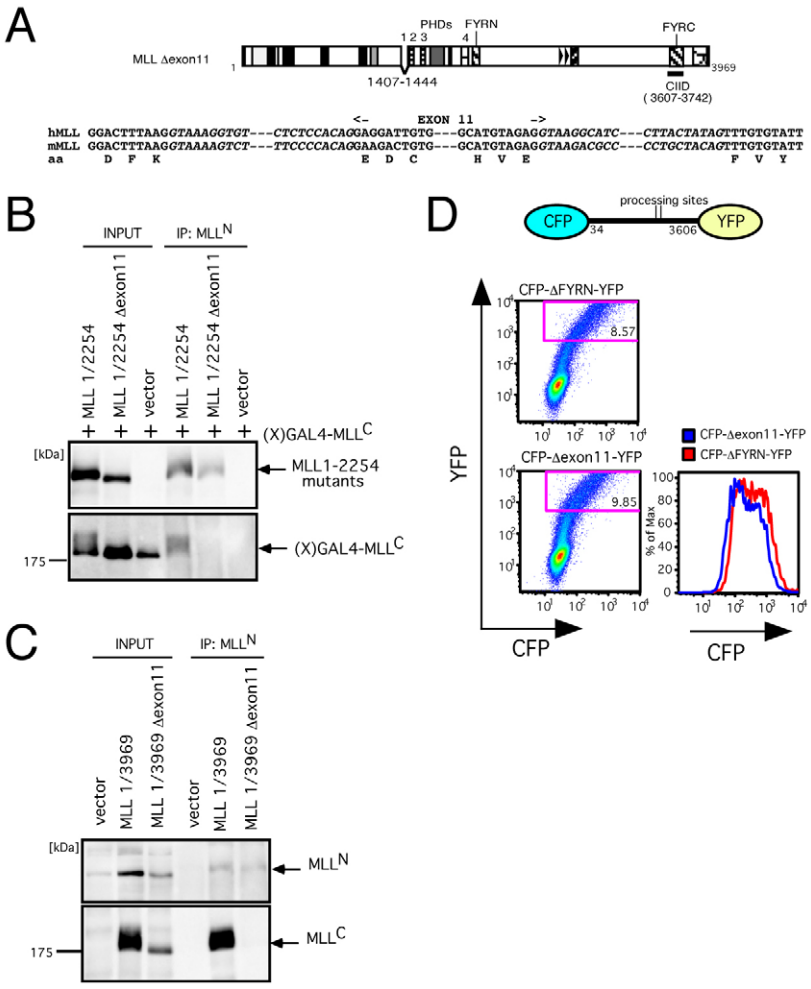

Fig. 5. The MLL Δexon11 mutant is incapable of forming an intramolecular MLL holocomplex and is susceptible to degradation. (**A**) Schematic representation of the Δexon11 mutant. The exon and intron structures around exon 11 are conserved between human (hMLL) and mouse (mMLL). (**B**) IP analysis was performed for the MLL 1/2254 Δexon11 mutant as in Fig. 4B. (**C**) IP analysis was performed for the MLL full-length Δexon11 mutant. IP analysis was performed for various MLL full-length Δexon11 tagged with an HA epitope at the C-terminus. MLL mutants were transiently expressed in 293T cells. The cell extracts were subjected to IP with anti-MLL^N (mmN4) antibody followed by immunoblotting. The precipitates and input samples, indicated on the top, were immunoblotted with anti-MLL^N (mmN4; top panel) and anti-HA(3F10) antibodies (bottom panel). (**D**) The stability of MLL^N Δexon11 was analyzed as in Fig. 4C.

localized MLL^C in the nucleus, suggesting that it contains nuclear export sequences that antagonize GAL4-mediated nuclear localization (Fig. 6B; supplementary material Fig. S1). Deletion of the transactivation and SET domains yielded more complete nuclear localization of GAL4–MLL^C proteins, implicating these domains in facilitating nuclear export (Fig. 6B). Coexpression of MLL^N and MLL^C resulted in nuclear colocalization of both subunits, whereas MLL^N containing the Δexon11 mutation failed to relocate MLL^C into the nucleus (Fig. 6C; supplementary material Fig. S1). Consistent with this notion, MLL^C derived from the Δexon11 mutant resided exclusively in the cytosolic fraction (Fig. 6D; supplementary material Fig. S1). These results suggest that MLL^N transports MLL^C into the nucleus through physical interaction, whereas MLL^C is actively exported to the cytosol if not anchored in the nucleus by MLL^N. Hence, the Δexon11 mutant is deficient for the MLL^C subunit.

The abundance of MLL^C proteins was markedly increased in the nuclear fraction when fused with GAL4 and additional nuclear localization signals (NLSs), indicating that MLL^C is relatively stable in the nucleus (Fig. 6E; supplementary material Fig. S1). Exogenously expressed MLL^C was markedly stabilized in the presence of MG132 proteasome inhibitor (Fig. 6F; supplementary material Fig. S1), whereas exogenously expressed MLL^N was unaffected, suggesting that the degradation mechanism of MLL^C is proteasome dependent but that of MLL^N is not. These results suggest that MLL^C is stable when associated with MLL^N in the nucleus, but is subjected to proteasome-dependent degradation in the cytosol when dissociated from MLL^N (Fig. 7).

Discussion

The MLL holocomplex is responsible for MLL-dependent transcription

Processing of MLL proteins is evolutionarily conserved; however, its consequences for MLL function are not well defined. Theoretically, processing enables production of free MLL^N, dissociated from MLL^C. To address the in vivo roles of MLL subunits, we created mutant mice that do not make MLL^C. *Mll^C*-deficient mice failed to maintain target gene expression and died during mid-gestation with an *Mll*-null phenotype demonstrating that MLL^C is required for the crucial transcriptional maintenance during embryogenesis.

MLL-dependent transcriptional maintenance was abolished in the *dC/dC* MEFs as expression of various MLL target genes was impaired and premature senescence was triggered. In human fibroblasts, MLL plays important roles in the maintenance of telomere integrity, and, therefore, knockdown of MLL induces the telomere-damage-response and p53-dependent senescence (Caslini et al., 2009). p53 activates expression of *PAI-1* in the induction of replicative senescence (Kortlever et al., 2006). Consistent with these notions, loss of MLL^C activates the p53–PAI-1 pathway

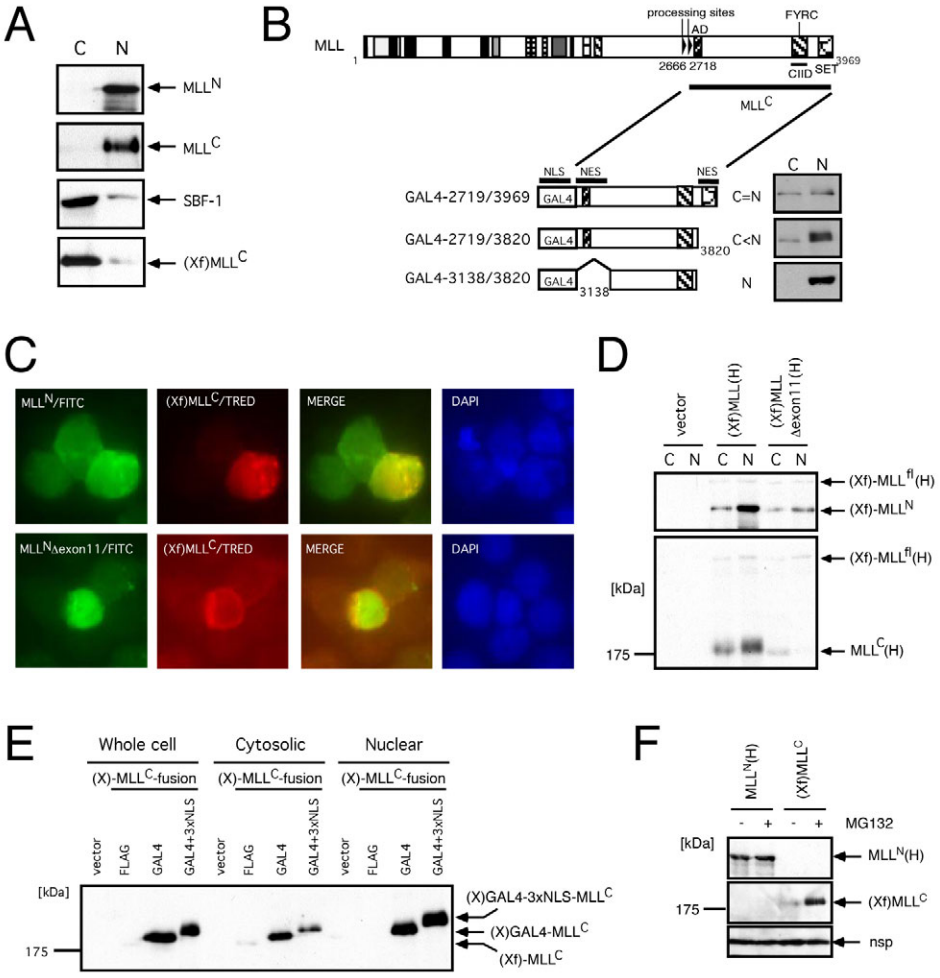

Fig. 6. MLL^C is exported to the cytosol after dissociation from MLL^N. (**A**) Subcellular localization of the endogenous MLL proteins and exogenous MLL^C. Xpress–FLAG-tagged (Xf) MLL^C (or vector) was transiently expressed in 293T cells that were lysed and separated into cytosolic (C) and nuclear (N) fractions and then immunoblotted for the indicated proteins with anti-MLL^N (mmN4.4), anti-MLL^C (mmC2.1), anti-SBF-1 (vector-transfected cells: upper three panels) or anti-Xpress antibodies [(Xf)MLL^C construct-transfected cells: bottom panel]. Sbf-1 served as a control for cytosolic localization. (**B**) Subcellular localization of various GAL4-MLL^C mutants. Various GAL4–MLL mutants, which are schematically illustrated, were analyzed for their subcellular localization as in A. GAL4 fusion proteins were visualized by anti-GAL4 antibody. (**C**) Colocalization of exogenous MLL^N or MLL^N Δexon11 with MLL^C. The indicated MLL^N mutants and (Xf)MLL^C fragments were coexpressed in 293T cells and analyzed by indirect immunofluorescence with anti-MLL^N (rpN1) and anti-Xpress antibodies. The MLL^N Δexon11 mutant served as a negative control. (**D**) Subcellular localization of exogenous full-length MLL proteins with or without the Δexon11 mutation. Full-length MLL tagged with Xpress and FLAG at its N-terminus and HA at its C-terminus [(Xf)MLL(H)] with or without deletion of exon 11 was analyzed as in A. Each fraction was immunoblotted with anti-Xpress or anti-HA antibody. (**E**) Expression of various MLL^C mutants driven by the same promoter and translation initiation sites with or without additional nuclear localization signals. (Xf)MLL^C, (X)GAL4–MLL^C, (X)GAL4–x3NLS–MLL^C were expressed in 293T cells, fractionated and immunoblotted with anti-Xpress antibody. (**F**) Sensitivities of MLL^N and MLL^C to the MG132 proteasome inhibitor. 293T cells were transfected with the corresponding expression vectors and cultured with and without 10 μM MG132 for 8 hours and subjected to western blotting with anti-Xpress antibody. A nonspecific band (nsp) serves as a loading control.

because *PAI-1* expression is induced in *dC/dC* MEFs, whereas the senescence phenotype can be rescued by a p53-null allele. Thus, MLL^C is required for MLL function in the maintenance of the cellular homeostasis of fibroblasts.

Analysis of fetal hematopoiesis shows that the MLL holocomplex is also required for hematopoietic development. It has been reported that MLL is required for reconstitution of the adult hematopoietic system by maintaining the propagation of myeloid progenitors and quiescence of HSCs, but not for differentiation (Ernst et al., 2004; Jude et al., 2007; McMahon et al., 2007; Yagi et al., 1998). Consistent with previous reports, fetal liver cells deficient for MLL^C had similar phenotypes. During hematopoietic development, MLL maintains expression of *Hoxa9* (Jude et al., 2007; Yagi et al., 1998), which is highly expressed in HSCs and MPPs and progressively downregulated in more differentiated progenitors (Forsberg et al., 2005; Krivtsov et al., 2006; Somervaille and Cleary, 2006). *Hoxa9* expression influences the proliferation status of undifferentiated hematopoietic cells because its forced expression expands the HSC or progenitor pools, including GMPs, whereas its loss produces the opposite effects (Kroon et al., 1998; Lawrence et al., 2005; Schnabel et al., 2000; Thorsteinsdottir et al., 2002; Wang et al., 2010a). MLL appears to maintain appropriate HSC pool sizes by sustaining *Hox* gene expression, the failure of which results in shortages of downstream

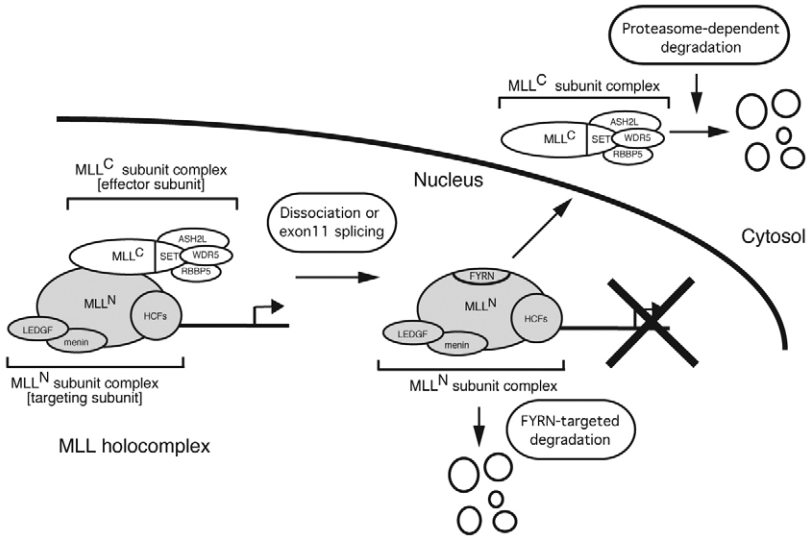

Fig. 7. A model of the two distinct degradation pathways for each MLL subunit.

progenitors and exhaustion of HSCs. Our analysis of the MLL-deficient hematopoietic system underscores a previously unappreciated role for MLL in LSK CD48^{+}Flk2^{+} cells, which is consistent with *Hoxa9* being most highly expressed in MPPs (Forsberg et al., 2005) and could account for the inability of *dC/dC* fetal liver cells to reconstitute the hematopoietic system, even short-term, despite seemingly intact differentiation capacities. Hence, MLL^{C} is crucial to early stages of hematopoietic development.

From these results we conclude that the MLL holocomplex is responsible for MLL-dependent transcription because MLL^{C} is required in three different biological processes including embryogenesis, maintenance of cellular homeostasis in fibroblasts and hematopoietic development.

MLL subunits are subjected to distinct degradation mechanisms upon dissociation

We observed that free Mll^{N} was undetectable in *dC* homozygous MEFs despite comparable expression of *Mll* mRNAs. Furthermore, *Mll^{C}*-deficient embryos expressed only minimal amounts of Mll^{N}. These results indicate that free MLL^{N} is degraded by a post-transcriptional mechanism in vivo. In this study, we discovered that free MLL^{C} is exported to the cytosol and degraded via a proteasome-dependent pathway. Thus, both of the MLL subunits generated by processing are unstable if not forming an MLL holocomplex. Free MLL^{N} is destroyed by a unique mechanism that targets the FYRN domain. This degradation mechanism appears to be independent of the proteasome degradation pathway and therefore should be different from the previously reported SCF- or APC-proteasome-dependent mechanisms that dynamically regulate MLL protein levels during the cell cycle, which targets a different portion of MLL (amino acids 1–1400) (Liu et al., 2007). It is unclear at this point how free MLL^{N} fragments are degraded. It might involve autophagic degradation similar to the piecemeal microautophagy of the nucleus observed in yeast (Krick et al., 2009) or 'nucleophagy' observed in mammalian cells (Park et al., 2009).

FYRN domains are often found adjacent to FYRC in SET domain-containing proteins and together constitute a DAST domain, which is evolutionarily conserved between humans and plants (Alvarez-Venegas and Avramova, 2001). The FYRN domain directly associates with the FYRC domain through the hydrophobic residues of each domain, thereby its interaction surface is kept unexposed (Garcia-Alai et al., 2010; Pless et al., 2011; Hsieh et al., 2003b). Our data suggest that the FYRN domain harbors a destabilization signal that is normally masked by MLL^{C} within the MLL holocomplex. Supporting this notion, deletion of FYRN did not render MLL^{N} unstable, despite an inability to associate with MLL^{C}. The ability of FYRN to destabilize the MLL-AF9 protein and inactivate its transcriptional and oncogenic properties is consistent with this proposal and probably accounts for the absence of chromosomal translocations downstream of the FYRN domain in human leukemias (Meyer et al., 2009). Hence, FYRN might serve not only as a platform for interaction with FYRC but also as a destabilization signal that activates the targeted destruction process when exposed. The exposed hydrophobic surface of FYRN might trigger aggregation of the free MLL^{N} fragment, which is then subjected to autophagic degradation (Knaevelsrud and Simonsen, 2010).

Because free MLL^{N} is degraded if it is dissociated from MLL^{C}, it is unlikely to possess any biological functions. However, free MLL^{N} might have functions in circumstances where the degradation pathway is inhibited. In *Drosophila*, it has been suggested that TRX^{N} associates with the genome without TRX^{C} at some loci. Whether MLL^{N} and MLL^{C} also differently associate with the human genome is currently unknown. Our data show that there is an intrinsic regulatory mechanism that effectively extinguishes MLL^{N} upon loss of intramolecular interaction. Therefore MLL^{N} must be protected from the degradation mechanism in order to function without MLL^{C} if it has a biological function (Fig. 7).

PHD1 is necessary for holocomplex formation and implicated in tumor suppression

Our structure–function analysis revealed that PHD1 and PHD4 are crucial for intramolecular interaction in the context of the full-length protein. PHD fingers serve as protein–protein interaction motifs (Fair et al., 2001). Recently, it has been shown that PHD3 specifically associates with di- and tri-methylated lysine 4 of histone H3 (Milne et al., 2010; Wang et al., 2010b; Chang et al., 2010). It is possible that PHD1 and/or PHD4 bind to specific motifs within MLL to enable or stabilize physical interaction between FYRN and FYRC. Such interactions could be modulated

through post-translational modifications such as lysine methylation, thereby providing opportunities for a context-dependent regulation of holocomplex formation.

We demonstrate here that exclusion of exon 11 sequences from the *MLL* mRNA produces a variant protein lacking PHD1 that is unable to associate with MLL^C, and thus subjected to degradation. Because the Δexon11 transcript is present in both normal and leukemia cells (Löchner et al., 1996; Nam et al., 1996; Takeuchi et al., 2008), alternative splicing of exon 11 might provide another context-dependent mechanism to conditionally extinguish MLL activity in vivo.

Genomic deletion and enhanced alternative splicing of *MLL* exon 11 have been reported in a subset of acute lymphoid leukemias (Löchner et al., 1996). Because exon 11 deletion abolishes holocomplex formation and renders MLL nonfunctional, its oncogenic mechanism should differ from MLL-fusion-associated leukemias, in which a gain-of-function mechanism plays the predominant role (Ayton and Cleary, 2001; Hess, 2004; Krivtsov and Armstrong, 2007). This raises the possibility that MLL serves as a tumor suppressor in the lymphoid lineage. In endocrine tissues, inactivating mutations of menin prevent the MLL–menin complex maintaining appropriate expression of *Cdkn1b* and *Cdkn2c* as part of a negative growth regulatory and tumor suppressor transcriptional circuit (Franklin et al., 1998; Franklin et al., 2000; Karnik et al., 2005; Milne et al., 2005). Indeed, these CDKIs are expressed at very low levels in *dC/dC* MEFs. These CDKIs have also been implicated in lymphoid growth control and tumorigenesis. Lymphoid cells from *Cdkn2c* knockout mice are hyper-proliferative to mitogens (Franklin et al., 1998), and inactivating mutations of *Cdkn1b* have been reported in T-ALL and other types of leukemia (Le Toriellec et al., 2008; Markaki et al., 2006). The Notch1 pathway, which is activated frequently in T-ALL, effectively reduces CDKN1B levels through upregulation of SKP2 expression (Dohda et al., 2007). Collectively, these data suggest that deletion of exon 11 might contribute to oncogenesis by downregulating CDKIs in lymphoid cells. Thus MLL might function as a tumor suppressor in the lymphoid lineage with a mechanism similar to that in endocrine tissues. However, conditional knockout studies show that *Mll* deficiency does not cause immediate expansion of lymphoid lineage populations (Jude et al., 2007; McMahon et al., 2007). These results do not support a rate-limiting role of MLL for proliferation of lymphoid cells, and suggest that additional mutations might be required for full transformation. Further investigation is required to determine whether MLL truly serves a tumor suppressor role in lymphoid lineages.

In summary, our studies define a crucial role for holocomplex formation of MLL subunits in various developmental processes, which is necessary to protect MLL^N from the FYRN-targeted degradation mechanism. Our data suggest that if MLL^N were to function without MLL^C, the FYRN domain must be masked or modified to ensure MLL^N stability; however, our studies provide no evidence for separate MLL^N function in various MLL-dependent processes.

Materials and Methods

Cell culture

293T, plat-E and MEF cells were cultured in Dulbecco's modified Eagle's medium supplemented with 15% fetal calf serum and non-essential amino acids.

Subfractionation, immunoprecipitation and western blotting

Preparation of nuclear extracts, immunoprecipitation (IP) and western blotting were performed as described previously (Yokoyama et al., 2004). Primary antibodies included mouse monoclonal anti-MLL^N (mmN4.4), anti-MLL^C (mmC2.1), anti-Sbf-1 (HAF3P.1) and polyclonal rabbit anti-MLL^N (rpN1) as described elsewhere (Yokoyama et al., 2002). Anti-HCF-1_C (H12) antibody was provided by Winship Herr. The mouse monoclonal anti-MLL^C (9–12) antibody was generated using maltose-binding protein (MBP) fusion protein corresponding to residues 3084–3959 of human MLL. Goat anti-menin (C19), mouse anti-GAL4 (RK5C1) and omni-probe (D-8; recognizes the nearby sequence of the Xpress epitope) antibodies were purchased from Santa Cruz Biotechnology, Inc. Additional primary antibodies included mouse anti-actin (MAB 1501R; Chemicon) and rat anti-HA (3F10; Roche). Agarose affinity beads coupled to mouse anti-FLAG (M2) monoclonal antibody were purchased from Sigma.

Construction of the expression vectors

Xpress–FLAG–MLL–HA expression vectors [pLNCX (Xf)MLL(H) and its derivatives] are described elsewhere (Yokoyama et al., 2002). Various MLL mutants were generated by polymerase chain reaction (PCR)-mediated mutagenesis and restriction enzyme digestion and/or ligation. The GAL4 DNA binding domain, Xpress epitope, 3xNLS and CFP and YFP portion were transferred from pM (Clontech), pcDNA4 Hix/Max (Invitrogen), pEF/myc/nuc/GFP (Invitrogen) and pECFP-C1/pEYFP-C1 (BD Biosciences) vectors, respectively. Assembled cDNAs were cloned into the pLNCX vector (Clontech). The various MLL-AF9 mutants were generated by modification of the pMSCV MLL-AF9 vector (Somervaille and Cleary, 2006).

Generation of knockin mice

A mouse ES BAC DNA pool (Down-to-the-well™) was screened by PCR to isolate a BAC clone containing the *Mll* locus. Targeting vectors containing neo and DT cassettes (kindly provided by Takeshi Yagi) were constructed by PCR-mediated mutagenesis, restriction enzyme digestion and ligation. ES cells (CGR8.8) were transfected with the linearized targeting vectors and screened for positive clones by PCR. Homologous recombination was confirmed by using the LA-PCR kit (Takara Bio Inc.) specific for both ends of the targeting construct (primer sequences available upon request). Targeted clones were transiently transfected with a Cre recombinase expression vector (kindly provided by Takeshi Yagi) and subsequently screened for clones with appropriate excision of the neo cassette. Diagnostic PCR for genotyping was performed using a primer pair of the forward primer: 5′-CTGGCATCATGTATTTTGAACAGGCACCCC-3′ and the reverse primer: 5′-TACACGTGGTAACCAGTCATCTGCAGCTCA-3′ by LA-PCR followed by digestion with *Xho*I. Blastocyst injections were performed by the Transgenic Research Facility of Stanford University. Germline transmission of the targeted *Mll* allele was confirmed by PCR genotype analysis. Knockin mouse lines were maintained by backcrossing onto a C57BL6 genetic background. p53 knockout mice were reported previously (Donehower et al., 1992).

Whole-mount in situ hybridization

In situ hybridization was performed on E10.5 embryos as described elsewhere (Capellini et al., 2006). Plasmids for probes were kindly provided by Licia Selleri.

Quantitative RT-PCR

Reverse transcription (RT) and quantitative PCR (qPCR) were performed as described previously (Yokoyama et al., 2005). Taqman probes for *Actb* (Mm00607939_s1), *Gapdh* (Mm99999915_g1), *Hoxa9* (Mm00439364_m1), *Hoxc4* (Mm00442838_m1), *Hoxc8* (Mm00439369_m1), *Hoxc9* (Mm00433972_m1), *Cdkn1b* (Mm00439167_g1), *Cdkn2c* (Mm00483243_m1), *Pml* (Mm00476969_m1), *Serpine1* (Mm00435860_m1), *Mll*(N) (Mm01179246_g1) and *Mll*(C) (Mm01179235_m1) were purchased from Applied Biosystems. qPCR was performed in triplicate and average expression levels (with standard deviations) normalized to that of *Gapdh* or β-actin gene were calculated using a standard curve and the relative quantification method as described in ABI User Bulletin #2.

MEF proliferation and 3T3 senescence assays

MEFs were derived from E11.5 embryos and handled as described elsewhere (Sage et al., 2000). In proliferation assay, 5×10^4 cells were plated in a 60 mm dish on day 0 and the cells were counted after trypsinization and resuspension in medium at each time point. In 3T3 senescence assays, 5×10^4 cells were replated in a 60 mm dish every 3 days.

Flow cytometry

Flow cytometry analysis was performed at the fluorescence-activated cell sorter (FACS) facility of Stanford University as previously described (Ficara et al., 2008). Fetal liver single-cell suspensions were stained in deficient Roswell Park Memorial Institute medium (RPMI; Irvine Scientific) containing 3% fetal calf serum, 1 mM EDTA and 0.01 M HEPES. Conjugated monoclonal antibodies were obtained from either BD Pharmingen (BD) or eBioscience (San Diego, CA). The lineage cocktail included Gr1 (RB6-8C5), B220 (RA3-6B2), TER119 (TER-119), CD3 (145-2C12), CD4 (GK1.5) and CD8. The following monoclonal antibodies were also used: Mac1/CD11b (M1/70), cKit (2B8), Sca1 (D7), CD48 (HM48-1), CD34 (49E8), CD16/32 (93), Flk2 (A2F10), CD45.2 (104) and CD43 (S7). Stained cells were analyzed with an LSR-1A or LSR-II flow cytometer. Cell Quest Pro or Diva (BD) were used for data acquisition, and FlowJo (Tree Star) was used for analysis.

Cytospin and in vitro differentiation to macrophages

Fetal liver cells were cultured for 1 week in methylcellulose medium (M3231; Stemcell Technologies; Vancouver, BC) containing SCF, IL-3, IL-6 and GM-CSF. Cytospin preparations were stained with May–Grunwald–Giemsa stain for assessment of cellular cytology as described elsewhere (Yokoyama et al., 2005).

In vivo reconstitution assay

Fetal liver cells from homozygous mutant (5×10^5 cells) or wt embryos (5×10^4 cells) were injected intravenously into lethally irradiated (900 rad) C57BL6 mice. Recipient mice were maintained on water supplemented with neomycin.

Myeloid progenitor transformation assay

The myeloid progenitor transformation assay was described elsewhere (Lavau et al., 1997; Yokoyama and Cleary, 2008). A portion of the cells was lysed at the end of the first round of plating to prepare RNA using an RNAeasy mini kit (Qiagen).

Indirect immunofluorescence

Indirect immunofluorescence was performed using 293T cells transfected with various *MLL* expression vectors as described elsewhere (Yokoyama and Cleary, 2008). Transfected cells were fixed and incubated with rabbit anti-MLL^N (rpN1) or mouse anti-Xpress (omni probe D-8) antibodies, and then probed with FITC-conjugated goat anti-rabbit IgG or TRED-conjugated anti-mouse IgG (Santa Cruz Biotechnology). Cells were stained with DAPI (Vector Laboratories) and analyzed by immunofluorescence microscopy.

We thank E. Allen and H. Zeng (Stanford Transgenic Research Facility) for technical support, T. Yagi and L. Selleri for plasmids, and W. Herr for an antibody. We acknowledge C. Nicolas, M. Ambrus, B. T. Rouse, C. Hatanaka and M. Kawaguchi for technical assistance, and A. James for graphics support. We thank L. Selleri, T. Capellini and J. Sage for technical instruction and helpful discussions. F.F. was supported by an ASH scholar award from the American Society of Hematology. These studies were supported by the Children's Health Initiative of the Packard Foundation and grants from the National Institutes of Health (CA55029 and CA116606) to M.L.C. and by a Grant-in-aid for Scientific Research on Innovative Areas (22118003) and a Grant-in-aid for the Third-Term Comprehensive 10-Year Strategy for Cancer Control to A.Y. Deposited in PMC for release after 12 months.

Supplementary material available online at
http://jcs.biologists.org/cgi/content/full/124/13/2208/DC1

References

Alvarez-Venegas, R. and Avramova, Z. (2001). Two Arabidopsis homologs of the animal trithorax genes: a new structural domain is a signature feature of the trithorax gene family. *Gene* **271**, 215-221.

Ayton, P. M. and Cleary, M. L. (2001). Molecular mechanisms of leukemogenesis mediated by MLL fusion proteins. *Oncogene* **20**, 5695-5707.

Ayton, P. M., Chen, E. H. and Cleary, M. L. (2004). Binding to nonmethylated CpG DNA is essential for target recognition, transactivation, and myeloid transformation by an MLL oncoprotein. *Mol. Cell. Biol.* **24**, 10470-10478.

Bertolino, P., Tong, W. M., Galendo, D., Wang, Z. Q. and Zhang, C. X. (2003). Heterozygous Men1 mutant mice develop a range of endocrine tumors mimicking multiple endocrine neoplasia type 1. *Mol. Endocrinol.* **17**, 1880-1892.

Birke, M., Schreiner, S., Garcia-Cuellar, M. P., Mahr, K., Titgemeyer, F. and Slany, R. K. (2002). The MT domain of the proto-oncoprotein MLL binds to CpG-containing DNA and discriminates against methylation. *Nucleic Acids Res.* **30**, 958-965.

Caldas, C., Kim, M. H., MacGregor, A., Cain, D., Aparicio, S. and Wiedemann, L. M. (1998). Isolation and characterization of a pufferfish MLL (mixed lineage leukemia)-like gene (fMll) reveals evolutionary conservation in vertebrate genes related to Drosophila trithorax. *Oncogene* **16**, 3233-3241.

Capellini, T. D., Di Giacomo, G., Salsi, V., Brendolan, A., Ferretti, E., Srivastava, D., Zappavigna, V. and Selleri, L. (2006). Pbx1/Pbx2 requirement for distal limb patterning is mediated by the hierarchical control of Hox gene spatial distribution and Shh expression. *Development* **133**, 2263-2273.

Caslini, C., Connelly, J. A., Serna, A., Broccoli, D. and Hess, J. L. (2009). MLL associates with telomeres and regulates telomeric repeat-containing RNA transcription. *Mol. Cell. Biol.* **29**, 4519-4526.

Chang, P. Y., Hom, R. A., Musselman, C. A., Zhu, L., Kuo, A., Gozani, O., Kutateladze, T. G. and Cleary, M. L. (2010). Binding of the MLL PHD3 finger to histone H3K4me3 is required for MLL-dependent gene transcription. *J. Mol. Biol.* **400**, 137-144.

Chen, J., Santillan, D. A., Koonce, M., Wei, W., Luo, R., Thirman, M. J., Zeleznik-Le, N. J. and Diaz, M. O. (2008). Loss of MLL PHD finger 3 is necessary for MLL-ENL-induced hematopoietic stem cell immortalization. *Cancer Res.* **68**, 6199-6207.

Christensen, J. L. and Weissman, I. L. (2001). Flk-2 is a marker in hematopoietic stem cell differentiation: a simple method to isolate long-term stem cells. *Proc. Natl. Acad. Sci. USA* **98**, 14541-14546.

Crabtree, J. S., Scacheri, P. C., Ward, J. M., Garrett-Beal, L., Emmert-Buck, M. R., Edgemon, K. A., Lorang, D., Libutti, S. K., Chandrasekharappa, S. C., Marx, S. J. et al. (2001). A mouse model of multiple endocrine neoplasia, type 1, develops multiple endocrine tumors. *Proc. Natl. Acad. Sci. USA* **98**, 1118-1123.

Dohda, T., Maljukova, A., Liu, L., Heyman, M., Grander, D., Brodin, D., Sangfelt, O. and Lendahl, U. (2007). Notch signaling induces SKP2 expression and promotes reduction of p27Kip1 in T-cell acute lymphoblastic leukemia cell lines. *Exp. Cell Res.* **313**, 3141-3152.

Donehower, L. A., Harvey, M., Slagle, B. L., McArthur, M. J., Montgomery, C. A., Jr, Butel, J. S. and Bradley, A. (1992). Mice deficient for p53 are developmentally normal but susceptible to spontaneous tumours. *Nature* **356**, 215-221.

Dou, Y., Milne, T. A., Ruthenburg, A. J., Lee, S., Lee, J. W., Verdine, G. L., Allis, C. D. and Roeder, R. G. (2006). Regulation of MLL1 H3K4 methyltransferase activity by its core components. *Nat. Struct. Mol. Biol.* **13**, 713-719.

Ernst, P., Fisher, J. K., Avery, W., Wade, S., Foy, D. and Korsmeyer, S. J. (2004). Definitive hematopoiesis requires the mixed-lineage leukemia gene. *Dev. Cell* **6**, 437-443.

Fair, K., Anderson, M., Bulanova, E., Mi, H., Tropschug, M. and Diaz, M. O. (2001). Protein interactions of the MLL PHD fingers modulate MLL target gene regulation in human cells. *Mol. Cell. Biol.* **21**, 3589-3597.

Ficara, F., Murphy, M. J., Lin, M. and Cleary, M. L. (2008). Pbx1 regulates self-renewal of long-term hematopoietic stem cells by maintaining their quiescence. *Cell Stem Cell* **2**, 484-496.

Forsberg, E. C., Prohaska, S. S., Katzman, S., Heffner, G. C., Stuart, J. M. and Weissman, I. L. (2005). Differential expression of novel potential regulators in hematopoietic stem cells. *PLoS Genet.* **1**, e28.

Franklin, D. S., Godfrey, V. L., Lee, H., Kovalev, G. I., Schoonhoven, R., Chen-Kiang, S., Su, L. and Xiong, Y. (1998). CDK inhibitors p18(INK4c) and p27(Kip1) mediate two separate pathways to collaboratively suppress pituitary tumorigenesis. *Genes Dev.* **12**, 2899-2911.

Franklin, D. S., Godfrey, V. L., O'Brien, D. A., Deng, C. and Xiong, Y. (2000). Functional collaboration between different cyclin-dependent kinase inhibitors suppresses tumor growth with distinct tissue specificity. *Mol. Cell. Biol.* **20**, 6147-6158.

Garcia-Alai, M. M., Allen, M. D., Joerger, A. C. and Bycroft, M. (2010). The structure of the FYR domain of transforming growth factor beta regulator 1. *Protein Sci.* **19**, 1432-1438.

Hess, J. L. (2004). MLL: a histone methyltransferase disrupted in leukemia. *Trends Mol. Med.* **10**, 500-507.

Hsieh, J. J., Cheng, E. H. and Korsmeyer, S. J. (2003a). Taspase1: a threonine aspartase required for cleavage of MLL and proper HOX gene expression. *Cell* **115**, 293-303.

Hsieh, J. J., Ernst, P., Erdjument-Bromage, H., Tempst, P. and Korsmeyer, S. J. (2003b). Proteolytic cleavage of MLL generates a complex of N- and C-terminal fragments that confers protein stability and subnuclear localization. *Mol. Cell. Biol.* **23**, 186-194.

Hughes, C. M., Rozenblatt-Rosen, O., Milne, T. A., Copeland, T. D., Levine, S. S., Lee, J. C., Hayes, D. N., Shanmugam, K. S., Bhattacharjee, A., Biondi, C. A. et al. (2004). Menin associates with a trithorax family histone methyltransferase complex and with the hoxc8 locus. *Mol. Cell* **13**, 587-597.

Jin, S., Zhao, H., Yi, Y., Nakata, Y., Kalota, A. and Gewirtz, A. M. (2010). c-Myb binds MLL through menin in human leukemia cells and is an important driver of MLL-associated leukemogenesis. *J. Clin. Invest.* **120**, 593-606.

Jude, C. D., Climer, L., Xu, D., Artinger, E., Fisher, J. K. and Ernst, P. (2007). Unique and independent roles for MLL in adult hematopoietic stem cells and progenitors. *Cell Stem Cell* **1**, 324-337.

Karnik, S. K., Hughes, C. M., Gu, X., Rozenblatt-Rosen, O., McLean, G. W., Xiong, Y., Meyerson, M. and Kim, S. K. (2005). Menin regulates pancreatic islet growth by promoting histone methylation and expression of genes encoding p27Kip1 and p18INK4c. *Proc. Natl. Acad. Sci. USA* **102**, 14659-14664.

Kim, I., He, S., Yilmaz, O. H., Kiel, M. J. and Morrison, S. J. (2006). Enhanced purification of fetal liver hematopoietic stem cells using SLAM family receptors. *Blood* **108**, 737-744.

Knaevelsrud, H. and Simonsen, A. (2010). Fighting disease by selective autophagy of aggregate-prone proteins. *FEBS Lett.* **584**, 2635-2645.

Kortlever, R. M., Higgins, P. J. and Bernards, R. (2006). Plasminogen activator inhibitor-1 is a critical downstream target of p53 in the induction of replicative senescence. *Nat. Cell Biol.* **8**, 877-884.

Krick, R., Muhe, Y., Prick, T., Bredschneider, M., Bremer, S., Wenzel, D., Eskelinen, E. L. and Thumm, M. (2009). Piecemeal microautophagy of the nucleus: genetic and morphological traits. *Autophagy* **5**, 270-272.

Krivtsov, A. V. and Armstrong, S. A. (2007). MLL translocations, histone modifications and leukaemia stem-cell development. *Nat. Rev. Cancer* **7**, 823-833.

Krivtsov, A. V., Twomey, D., Feng, Z., Stubbs, M. C., Wang, Y., Faber, J., Levine, J. E., Wang, J., Hahn, W. C., Gilliland, D. G. et al. (2006). Transformation from committed progenitor to leukaemia stem cell initiated by MLL-AF9. *Nature* **442**, 818-822.

Kroon, E., Krosl, J., Thorsteinsdottir, U., Baban, S., Buchberg, A. M. and Sauvageau, G. (1998). Hoxa9 transforms primary bone marrow cells through specific collaboration with Meis1a but not Pbx1b. *EMBO J.* **17**, 3714-3725.

Lavau, C., Szilvassy, S. J., Slany, R. and Cleary, M. L. (1997). Immortalization and leukemic transformation of a myelomonocytic precursor by retrovirally transduced HRX-ENL. *EMBO J.* **16**, 4226-4237.

Lawrence, H. J., Christensen, J., Fong, S., Hu, Y. L., Weissman, I., Sauvageau, G., Humphries, R. K. and Largman, C. (2005). Loss of expression of the Hoxa-9

homeobox gene impairs the proliferation and repopulating ability of hematopoietic stem cells. *Blood* **106**, 3988-3994.

Le Toriellec, E., Despouy, G., Pierron, G., Gaye, N., Joiner, M., Bellanger, D., Vincent-Salomon, A. and Stern, M. H. (2008). Haploinsufficiency of CDKN1B contributes to leukemogenesis in T-cell prolymphocytic leukemia. *Blood* **111**, 2321-2328.

Liu, H., Cheng, E. H. and Hsieh, J. J. (2007). Bimodal degradation of MLL by SCFSkp2 and APCCdc20 assures cell cycle execution: a critical regulatory circuit lost in leukemogenic MLL fusions. *Genes Dev.* **21**, 2385-2398.

Löchner, K., Siegler, G., Fuhrer, M., Greil, J., Beck, J. D., Fey, G. H. and Marschalek, R. (1996). A specific deletion in the breakpoint cluster region of the ALL-1 gene is associated with acute lymphoblastic T-cell leukemias. *Cancer Res.* **56**, 2171-2177.

Mansson, R., Hultquist, A., Luc, S., Yang, L., Anderson, K., Kharazi, S., Al-Hashmi, S., Liuba, K., Thoren, L., Adolfsson, J. et al. (2007). Molecular evidence for hierarchical transcriptional lineage priming in fetal and adult stem cells and multipotent progenitors. *Immunity* **26**, 407-419.

Markaki, E. A., Stiakaki, E., Zafiropoulos, A., Arvanitis, D. A., Katzilakis, N., Dimitriou, H., Spandidos, D. A. and Kalmanti, M. (2006). Mutational analysis of the cell cycle inhibitor Kip1/p27 in childhood leukemia. *Pediatr. Blood Cancer* **47**, 14-21.

McMahon, K. A., Hiew, S. Y., Hadjur, S., Veiga-Fernandes, H., Menzel, U., Price, A. J., Kioussis, D., Williams, O. and Brady, H. J. (2007). Mll has a critical role in fetal and adult hematopoietic stem cell self-renewal. *Cell Stem Cell* **1**, 338-345.

Meyer, C., Kowarz, E., Hofmann, J., Renneville, A., Zuna, J., Trka, J., Ben Abdelali, R., Macintyre, E., De Braekeleer, E., De Braekeleer, M. et al. (2009). New insights to the MLL recombinome of acute leukemias. *Leukemia* **23**, 1490-1499.

Milne, T. A., Briggs, S. D., Brock, H. W., Martin, M. E., Gibbs, D., Allis, C. D. and Hess, J. L. (2002). MLL targets SET domain methyltransferase activity to Hox gene promoters. *Mol. Cell* **10**, 1107-1117.

Milne, T. A., Hughes, C. M., Lloyd, R., Yang, Z., Rozenblatt-Rosen, O., Dou, Y., Schnepp, R. W., Krankel, C., Livolsi, V. A., Gibbs, D. et al. (2005). Menin and MLL cooperatively regulate expression of cyclin-dependent kinase inhibitors. *Proc. Natl. Acad. Sci. USA* **102**, 749-754.

Milne, T. A., Kim, J., Wang, G. G., Stadler, S. C., Basrur, V., Whitcomb, S. J., Wang, Z., Ruthenburg, A. J., Elenitoba-Johnson, K. S., Roeder, R. G. et al. (2010). Multiple interactions recruit MLL1 and MLL1 fusion proteins to the HOXA9 locus in leukemogenesis. *Mol. Cell* **38**, 853-863.

Muntean, A. G., Giannola, D., Udager, A. M. and Hess, J. L. (2008). The PHD fingers of MLL block MLL fusion protein-mediated transformation. *Blood* **112**, 4690-4693.

Muntean, A. G., Tan, J., Sitwala, K., Huang, Y., Bronstein, J., Connelly, J. A., Basrur, V., Elenitoba-Johnson, K. S. and Hess, J. L. (2010). The PAF complex synergizes with MLL fusion proteins at HOX loci to promote leukemogenesis. *Cancer Cell* **17**, 609-621.

Nakamura, T., Mori, T., Tada, S., Krajewski, W., Rozovskaia, T., Wassell, R., Dubois, G., Mazo, A., Croce, C. M. and Canaani, E. (2002). ALL-1 is a histone methyltransferase that assembles a supercomplex of proteins involved in transcriptional regulation. *Mol. Cell* **10**, 1119-1128.

Nam, D. K., Honoki, K., Yu, M. and Yunis, J. J. (1996). Alternative RNA splicing of the MLL gene in normal and malignant cells. *Gene* **178**, 169-175.

Park, Y. E., Hayashi, Y. K., Bonne, G., Arimura, T., Noguchi, S., Nonaka, I. and Nishino, I. (2009). Autophagic degradation of nuclear components in mammalian cells. *Autophagy* **5**, 795-804.

Pless, B., Oehm, C., Knauer, S., Stauber, R. H., Dingermann, T. and Marschalek, R. (2011). The heterodimerization domains of MLL-FYRN and FYRC-are potential target structures in t(4;11) leukemia. *Leukemia* **25**, 663-670.

Sage, J., Mulligan, G. J., Attardi, L. D., Miller, A., Chen, S., Williams, B., Theodorou, E. and Jacks, T. (2000). Targeted disruption of the three Rb-related genes leads to loss of G(1) control and immortalization. *Genes Dev.* **14**, 3037-3050.

Schnabel, C. A., Jacobs, Y. and Cleary, M. L. (2000). HoxA9-mediated immortalization of myeloid progenitors requires functional interactions with TALE cofactors Pbx and Meis. *Oncogene* **19**, 608-616.

Schuettengruber, B., Ganapathi, M., Leblanc, B., Portoso, M., Jaschek, R., Tolhuis, B., van Lohuizen, M., Tanay, A. and Cavalli, G. (2009). Functional anatomy of polycomb and trithorax chromatin landscapes in Drosophila embryos. *PLoS Biol.* **7**, e13.

Silver, P. A., Keegan, L. P. and Ptashne, M. (1984). Amino terminus of the yeast GAL4 gene product is sufficient for nuclear localization. *Proc. Natl. Acad. Sci. USA* **81**, 5951-5955.

Somervaille, T. C. and Cleary, M. L. (2006). Identification and characterization of leukemia stem cells in murine MLL-AF9 acute myeloid leukemia. *Cancer Cell* **10**, 257-268.

Southall, S. M., Wong, P. S., Odho, Z., Roe, S. M. and Wilson, J. R. (2009). Structural basis for the requirement of additional factors for MLL1 SET domain activity and recognition of epigenetic marks. *Mol. Cell* **33**, 181-191.

Steward, M. M., Lee, J. S., O'Donovan, A., Wyatt, M., Bernstein, B. E. and Shilatifard, A. (2006). Molecular regulation of H3K4 trimethylation by ASH2L, a shared subunit of MLL complexes. *Nat. Struct. Mol. Biol.* **13**, 852-854.

Takeuchi, M., Nakaseko, C., Miyagi, S., Takeda, Y., Ozawa, S., Ohwada, C., Cho, R., Nishimura, M., Saito, Y. and Iwama, A. (2008). Clonal expansion of non-leukemic cells expressing two novel MLL-ELL variants differing in transforming activity. *Leukemia* **22**, 861-864.

Thorsteinsdottir, U., Mamo, A., Kroon, E., Jerome, L., Bijl, J., Lawrence, H. J., Humphries, K. and Sauvageau, G. (2002). Overexpression of the myeloid leukemia-associated Hoxa9 gene in bone marrow cells induces stem cell expansion. *Blood* **99**, 121-129.

Wang, Y., Krivtsov, A. V., Sinha, A. U., North, T. E., Goessling, W., Feng, Z., Zon, L. I. and Armstrong, S. A. (2010a). The Wnt/beta-catenin pathway is required for the development of leukemia stem cells in AML. *Science* **327**, 1650-1653.

Wang, Z., Song, J., Milne, T. A., Wang, G. G., Li, H., Allis, C. D. and Patel, D. J. (2010b). Pro isomerization in MLL1 PHD3-bromo cassette connects H3K4me readout to CyP33 and HDAC-mediated repression. *Cell* **141**, 1183-1194.

Yagi, H., Deguchi, K., Aono, A., Tani, Y., Kishimoto, T. and Komori, T. (1998). Growth disturbance in fetal liver hematopoiesis of Mll-mutant mice. *Blood* **92**, 108-117.

Yokoyama, A. and Cleary, M. L. (2008). Menin critically links MLL proteins with LEDGF on cancer-associated target genes. *Cancer Cell* **14**, 36-46.

Yokoyama, A., Kitabayashi, I., Ayton, P. M., Cleary, M. L. and Ohki, M. (2002). Leukemia proto-oncoprotein MLL is proteolytically processed into 2 fragments with opposite transcriptional properties. *Blood* **100**, 3710-3718.

Yokoyama, A., Wang, Z., Wysocka, J., Sanyal, M., Aufiero, D. J., Kitabayashi, I., Herr, W. and Cleary, M. L. (2004). Leukemia proto-oncoprotein MLL forms a SET1-like histone methyltransferase complex with menin to regulate Hox gene expression. *Mol. Cell. Biol.* **24**, 5639-5649.

Yokoyama, A., Somervaille, T. C., Smith, K. S., Rozenblatt-Rosen, O., Meyerson, M. and Cleary, M. L. (2005). The menin tumor suppressor protein is an essential oncogenic cofactor for MLL-associated leukemogenesis. *Cell* **123**, 207-218.

Yu, B. D., Hess, J. L., Horning, S. E., Brown, G. A. and Korsmeyer, S. J. (1995). Altered Hox expression and segmental identity in Mll-mutant mice. *Nature* **378**, 505-508.

Yu, B. D., Hanson, R. D., Hess, J. L., Horning, S. E. and Korsmeyer, S. J. (1998). MLL, a mammalian trithorax-group gene, functions as a transcriptional maintenance factor in morphogenesis. *Proc. Natl. Acad. Sci. USA* **95**, 10632-10636.

Zeleznik-Le, N. J., Harden, A. M. and Rowley, J. D. (1994). 11q23 translocations split the "AT-hook" cruciform DNA-binding region and the transcriptional repression domain from the activation domain of the mixed-lineage leukemia (MLL) gene. *Proc. Natl. Acad. Sci. USA* **91**, 10610-10614.

Journal of Cell Science

Figure S1

Graphical representations of various constructs used in the manuscript.

MLL mutant proteins are shown schematically and grouped according to the experiments in which they were employed and the relevant figure numbers in the main text: (A) proteins shown in Fig. 4A and B, (B) Fig. 4C, (C) Fig. 4E and F, (D) Fig. 5B, (E) Fig. 5C, (F) Fig. 5D, (G) Fig. 6A, (H) Fig. 6B, (I) Fig. 6C, (J) Fig. 6D, (K) Fig. 6E, and (L) Fig. 6F. Predicted molecular mass (kDa) of each mutant is shown on the right.

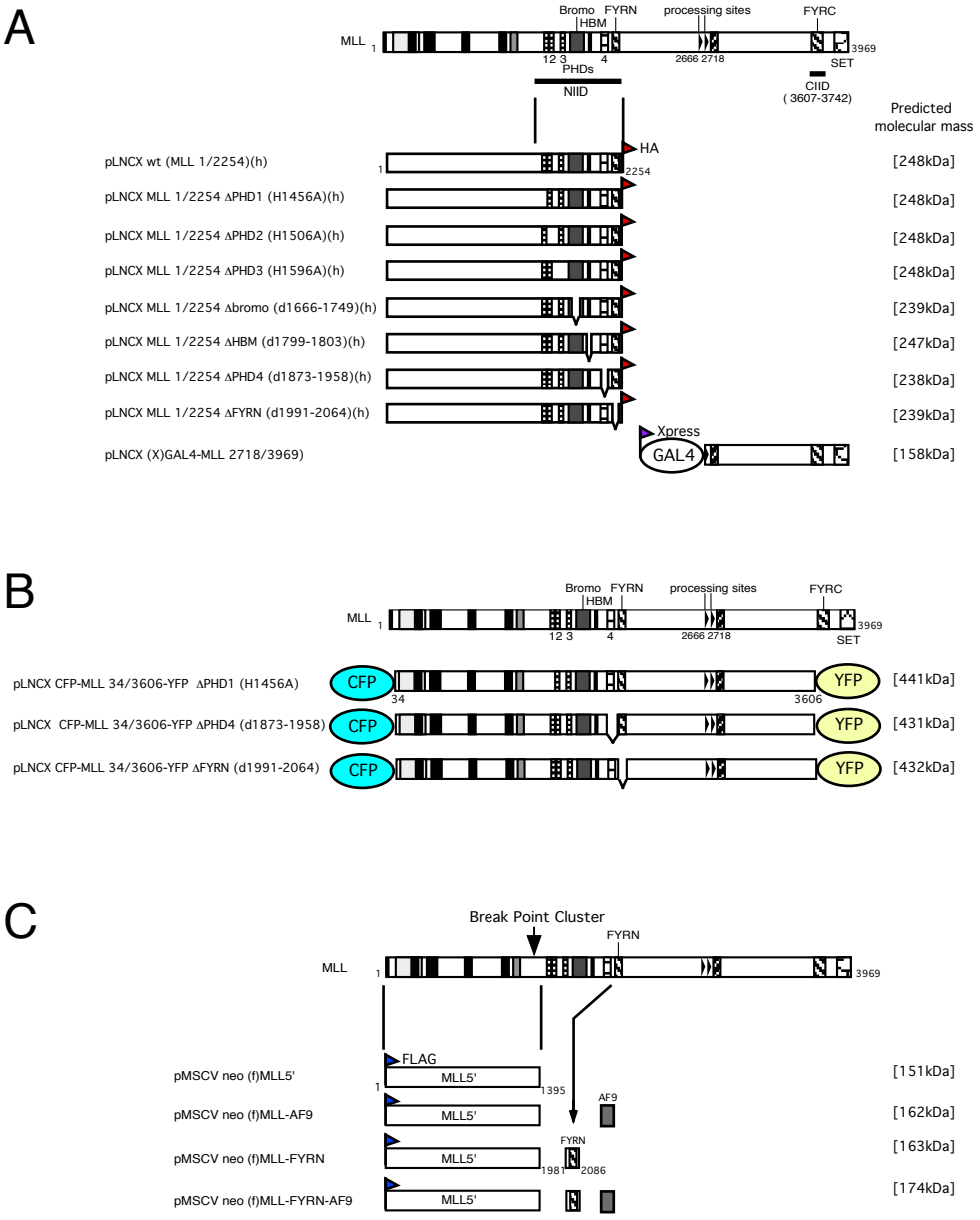

Figure S1 continued

D

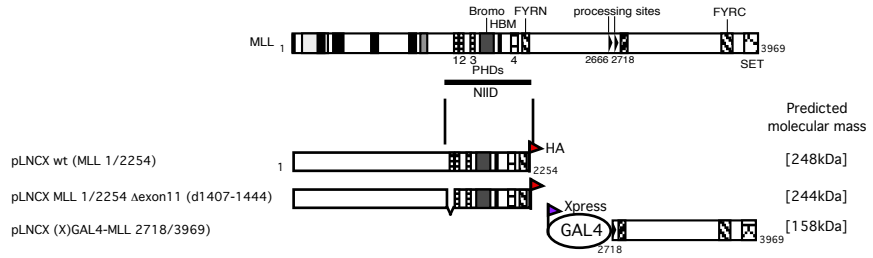

E

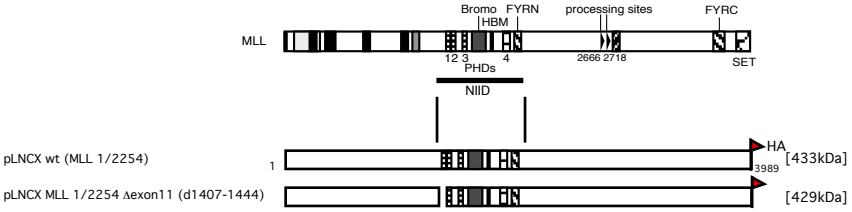

F

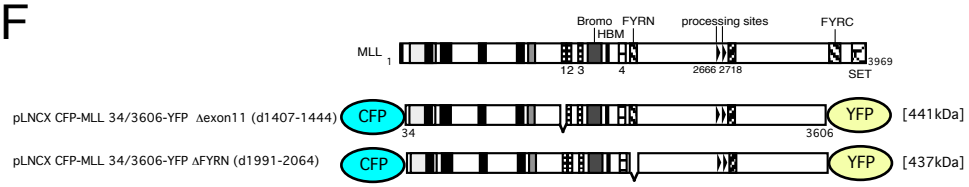

Figure S1 continued

G

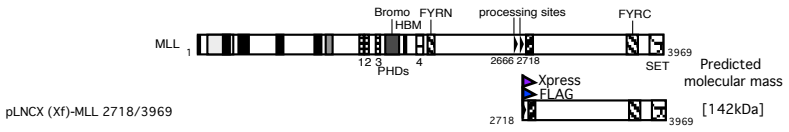

H

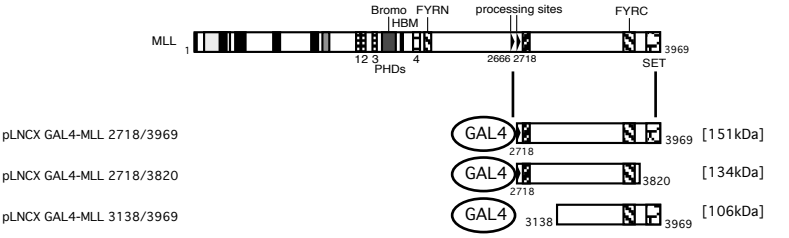

I

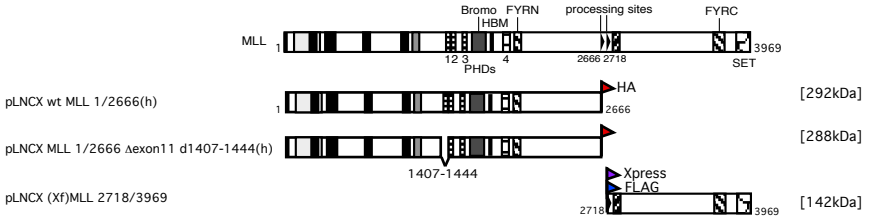

J

K

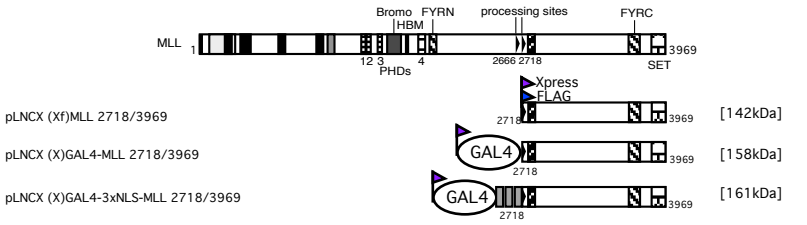

L

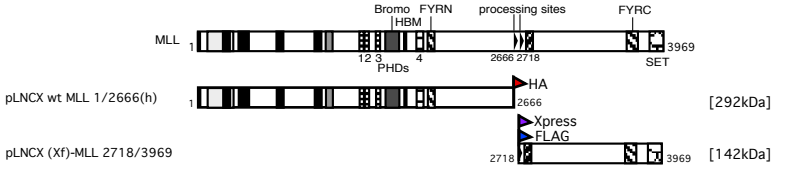

Figure S2

MLL mutants that do not associate with MLL^C can interact with HCF-1.

A. Schematic representation of the mutants. Predicted molecular mass of each mutant is shown on the right.

B. IP-western blot analysis was performed for various MLL 1/2254 mutants that do not associate with MLL^C. MLL 1/2254 mutants were transiently expressed in 293T cells. The cell extracts were subjected to immunoprecipitation (IP) with anti-HA (3F10) antibody followed by immunoblotting. The precipitates and input samples indicated on the top were immunoblotted with anti-HA (top panel) or anti-HCF-1C (H12) (bottom panel) antibodies.

C. IP-western blot analysis was performed for MLL1/2254 Δexon11 mutant as in panel B. HCF-1 binding was observed for the Δexon11 mutant.

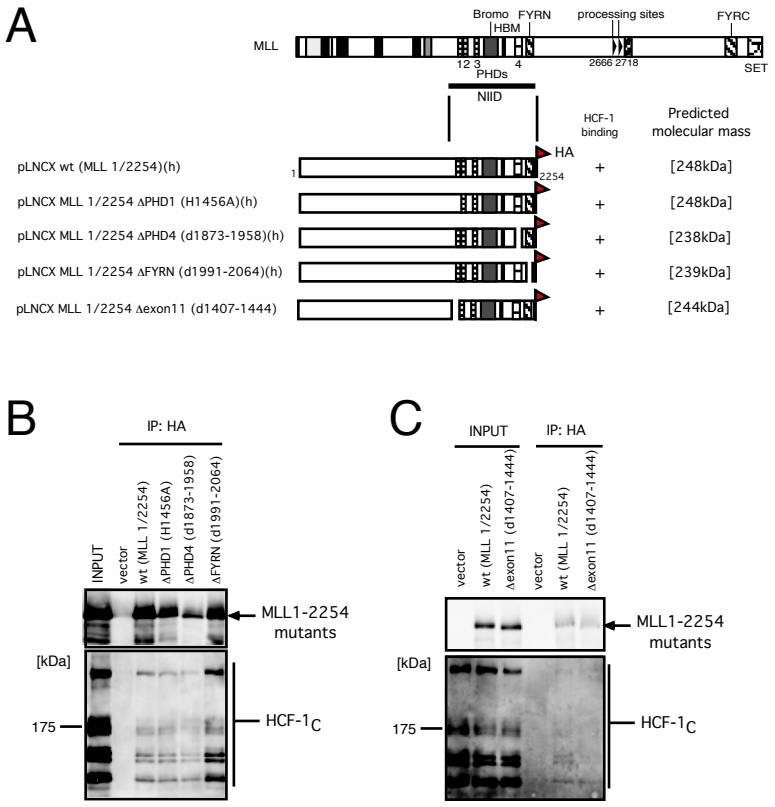

Figure S1

Graphical representations of various constructs used in the manuscript.

MLL mutant proteins are shown schematically and grouped according to the experiments in which they were employed and the relevant figure numbers in the main text: (A) proteins shown in Fig. 4A and B, (B) Fig. 4C, (C) Fig. 4E and F, (D) Fig. 5B, (E) Fig. 5C, (F) Fig. 5D, (G) Fig. 6A, (H) Fig. 6B, (I) Fig. 6C, (J) Fig. 6D, (K) Fig. 6E, and (L) Fig. 6F. Predicted molecular mass (kDa) of each mutant is shown on the right.

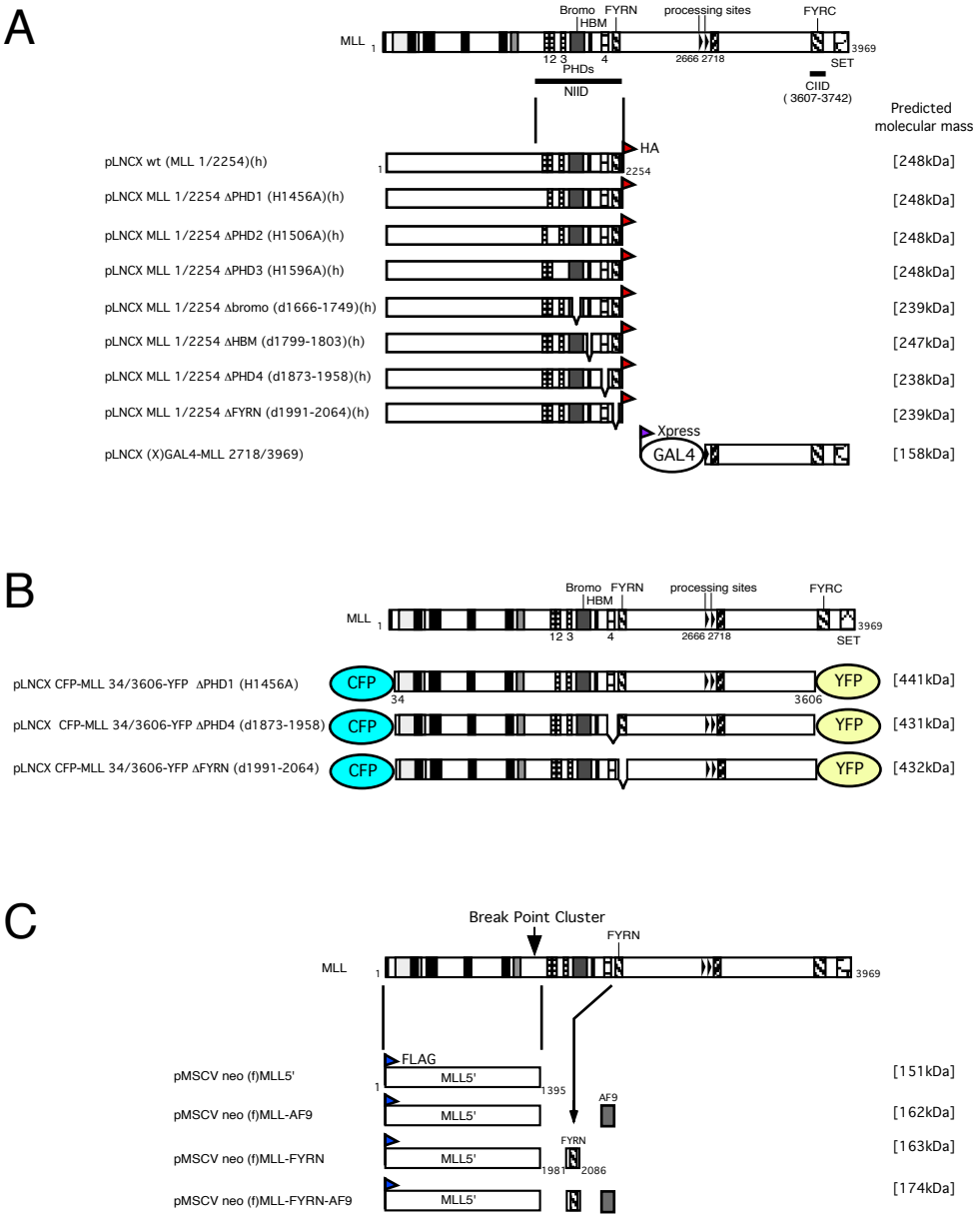

Figure S1 continued

D

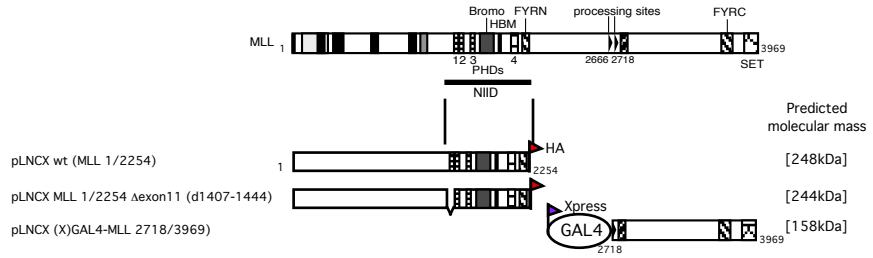

E

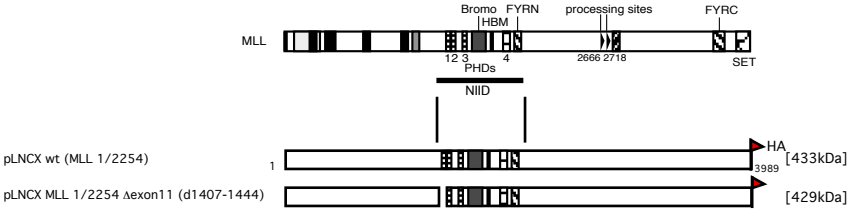

F

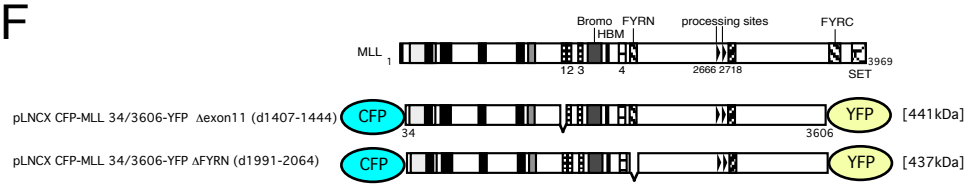

Figure S1 continued

G

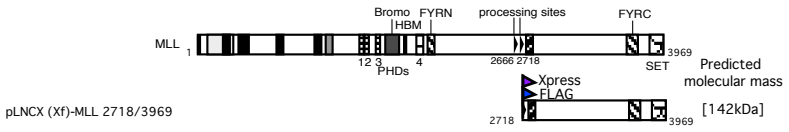

H

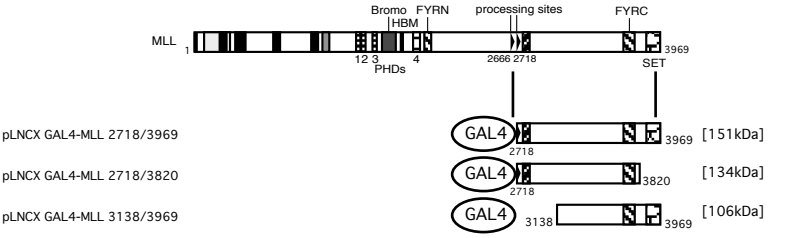

I

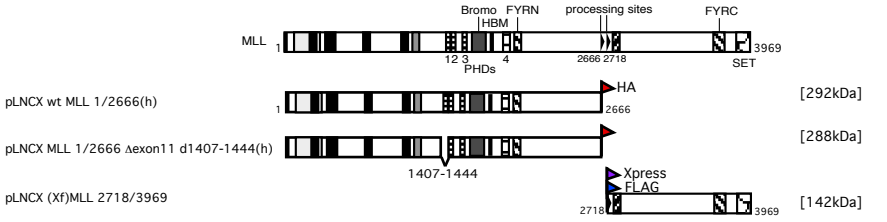

J

K

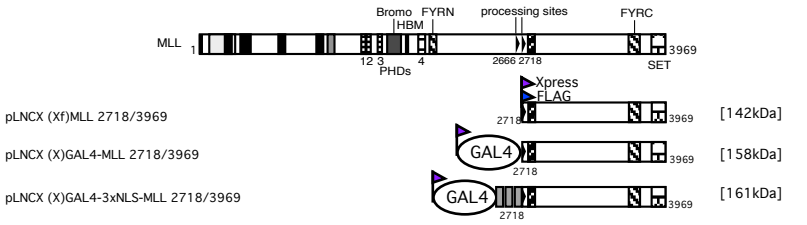

L

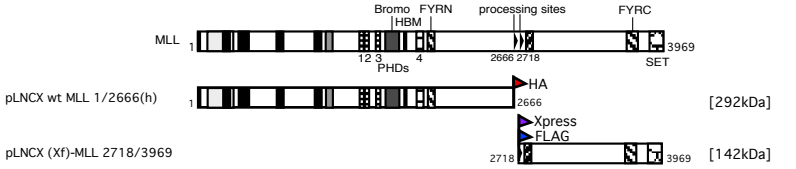

Figure S2

MLL mutants that do not associate with MLL^C can interact with HCF-1.

A. Schematic representation of the mutants. Predicted molecular mass of each mutant is shown on the right.

B. IP-western blot analysis was performed for various MLL 1/2254 mutants that do not associate with MLL^C. MLL 1/2254 mutants were transiently expressed in 293T cells. The cell extracts were subjected to immunoprecipitation (IP) with anti-HA (3F10) antibody followed by immunoblotting. The precipitates and input samples indicated on the top were immunoblotted with anti-HA (top panel) or anti-HCF-1C (H12) (bottom panel) antibodies.

C. IP-western blot analysis was performed for MLL1/2254 Δexon11 mutant as in panel B. HCF-1 binding was observed for the Δexon11 mutant.

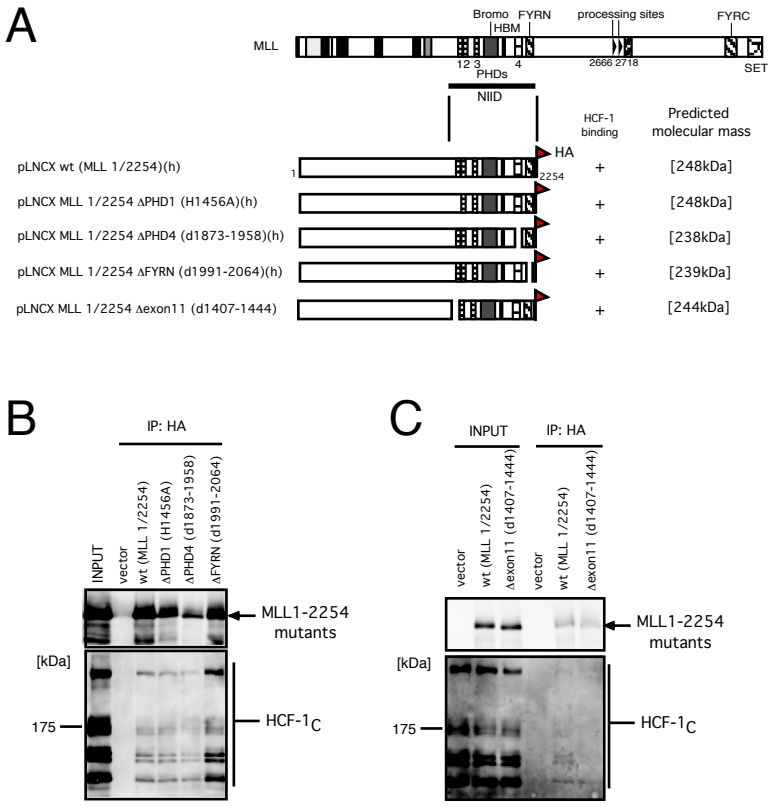

Figure S3

The FYRN domain is required for holocomplex formation and destabilization in various contexts.

A. Schematic representation of the full-length MLL mutants. Binding property with MLL^C, susceptibility to destabilization, and predicted molecular mass of each mutant are shown on the right.

B. IP-western blot analysis was performed for various MLL full-length mutants tagged with an HA epitope at the C-terminus. MLL mutants were transiently expressed in 293T cells. The cell extracts were subjected to IP with anti-MLL^N antibody (mmN4) followed by immunoblotting. The precipitates and input samples indicated on the top were immunoblotted with anti-MLL^N (mmN4) (top panel) or anti-HA (3F10) (bottom panel) antibodies.

C. Schematic representation of the various MLL deletion mutants. Binding property with MLL^C, susceptibility to destabilization, and predicted molecular mass of each mutant are shown on the right.

D. IP-western blot analysis was performed for various MLL deletion mutants as in Figure 4B. MLL deletion mutants were co-expressed with Xpress-tagged GAL4-MLL^C [(X) GAL4-MLL^C] in 293T cells. The cell extracts were subjected to IP with anti-MLL^N (mmN4) antibody, and the precipitates and input samples indicated at the top were immunoblotted with anti-MLL^N (mmN4) (top panel) or anti-Xpress (middle bottom two panels) antibodies.